



Research paper

A new smart charging electric vehicle and optimal DG placement in active distribution networks with optimal operation of batteries

Bilal Naji Alhasnawi ^{a,*} , Marek Zanker ^b, Vladimír Bureš ^{b,*} ^a Department of Fuel and Energy Techniques Engineering, Petroleum and Energy Engineering Technical College, Al-Furat Al-Awsat Technical University, Kufa, 66001, Iraq^b Faculty of Informatics and Management, University of Hradec Králové, 50003, Hradec Králové, Czech Republic

ARTICLE INFO

ABSTRACT

Keywords:
 IEEE 85-bus distributed network
 IEEE 33-bus distribution network
 Batteries
 Electric vehicles
 Optimization algorithms

The idea of Distribution Networks (DNs) is being developed to automate networks and better integrate renewable energy sources. To do this, the DNs integrate energy storage systems with Distributed Generating Units (DGs). This research report attempts to accomplish too many goals at once. In order to reduce MGs' reliance on the main grid, this study first proposes a smart charging method for PHEVs that maximizes the utilization of RERs and DERs while minimizing the amount of energy taken from the main grid. Second, the issue of how to best operate lithium-ion batteries to raise the technical, financial, and environmental indices of both independent and grid-connected distribution networks is addressed in this work. Thirdly, this paper proposes an optimization technique based on the Mountain Gazelle Optimizer (MGO), Improved Beluga Whale Optimization (IBWO), and Arithmetic Optimization Algorithm (AOA) for determining the optimal DGs in radial distribution systems. The effectiveness of the suggested framework is tested on IEEE 33-bus and IEEE 85-bus systems, and the findings demonstrate that, in spite of the complexity that arises from changing situations, the model offers an effective restoration solution. The proposed method finds reductions of about 6.83 % in power losses using AOA, reductions of about 17.92 % in power losses using IBWO, reductions of about 22.69 % in power losses and reductions of about 25.43 % in CO₂ emissions using MGO, when compared to the benchmark case in the IEEE 33-bus network, whereas the proposed method finds reductions of about 1.31 % in power losses using AOA, reductions of about 15.85 % in power losses using IBWO, reductions of about 19.48 % in power losses and reductions of about 23.27 % in CO₂ emissions using MGO, when compared to the benchmark case in the IEEE 85-bus network.

1. Introduction

Because it releases CO₂ and significantly raises temperatures, the overuse of conventional vehicles has a negative effect on the environment. It impacts the biological system and causes global warming. Most individuals use gasoline-powered vehicles for their daily commutes. A multitude of factors, such as environmental contamination and rising oil prices, stimulate the use of alternative modes of transportation. By using EVs, fossil fuels will be conserved and the issues with the traditional transportation system will be lessened. Many countries around the world are moving to battery-powered vehicles in an effort to cut pollution. EVs must connect to the power network in order to charge their batteries. Grid operations are facing significant hurdles as a result of the EVs' explosive expansion. Furthermore, more reliable Electric Vehicle

Charging Station (EVCS) systems are required as the number of EVs produced increases. When EVs are connected to the grid, the generation-demand balance is impacted and system load is increased. The electrical grid's ability to function smoothly may be significantly impacted by harmonics, increased power loss, and voltage fluctuations caused by improper charging station siting. Over the past ten years, there has been an increase in the significance of research on the ideal location for connecting EVCS and its load demand on the grid. The EVCS placement challenge was developed with consideration for driver comfort and charging station accessibility. There is discussion on the benefits of EVCS distribution on different busses. In [1], the configuration of various EVCS kinds and the optimization of the size of residential and commercial entities, offices, and homes inside the grid were covered.

On the other hand, because of the exponential growth in power system demand, power utilities are confronting significant difficulties.

* Corresponding authors.

E-mail addresses: bilalnaji11@yahoo.com (B.N. Alhasnawi), vladimir.bures@uhk.cz (V. Bureš).

Nomenclature		Variables & Parameters
<i>Abbreviations & Acronyms</i>		
DNs	Distribution Networks	\mathcal{P}_{pv} Output Power of solar
DGs	Distributed Generating units	T_c Module Temperature
PHEVs	Plug-In Hybrid Electric Vehicles	I_{rad} Solar irradiance
RERs/DERs	Renewable/Distributed Energy Resources	$P_B^{dis}(t)$ Power Discharge Battery
MGO	Mountain Gazelle Optimizer	η_{dis}, η_{ch} discharging and charging battery efficiency
IBWO	Improved Beluga Whale Optimization	P_B^{\max} Maximum power
AOA	Arithmetic Optimization Algorithm	$\mu_B(t)$ Binary variable of battery
EVs	Electric Vehicle	β^{ch} Influence factors of PEV charging
EVCS	Electric Vehicle Charging Station	β^{dis} Influence factors of PEV discharging
μ -PMU	Micro-Phasor Measurement Unit	P_{DER}, P_{PHEV} , and $P_{Load}(t)$ output power of RERs/DERs, PHEV power, and load power
DNN	Deep Neural Network	E_{ex} energy exchanged with utility grid.
SCADA	Supervisory Control and Data Acquisition	$P_{grid}(t), P_{Load}(t)$ and $P_{Loss}(t)$ utility grid power, load power and losses power
MPPT	Maximum Power Point Tracking	V_n^{\min} minimum voltage
EMS	Energy Management System	V_n^{\max} maximum voltage
ZOA	Zebra Optimization Algorithm	N number of buses
GNDO	Generalized Normal Distribution Optimizer	$V_{n,t}$ voltage at bus n
PV-STATCOM	Photovoltaic Static Synchronous Compensator	$P_{DER_i}^{\max}$ and $P_{DER_i}^{\min}$ maximum and minimum on DER active power
PMU	Phasor Measurement Unit	$P_{Diesel}^{\max}, P_{WT}^{\max}$, and P_{pv}^{\max} diesel generators, WT's, and PV array's respective maximum output
PEVs	Plug-in Electric Vehicles	$Q_{DER_i}^{\min}$ and $Q_{DER_i}^{\max}$ maximum and minimum on DER reactive power
DSO	Distribution System Operator	x_{T+1} Beluga position
DISCO	Distribution Company	h boundary constant
LSF	Loss Sensitivity Factor	r randomly chosen beluga whale
CBs	Capacitor Banks	$male_{gazelle}$ best global solution position vector
G2V	Grid to Vehicles	M_{pr} average number of search agents
V2G	Vehicles to Grid	X_{ra} random solution in interval of ra
GCN	Grid-Connected Network	$MaxIter$ total number of iterations
RGT	Renewable Generation Technology	$Iter$ number of iterations that are currently occurring
SN	Standalone Network	X_{rand} vector location of a randomly chosen gazelle
EST	Energy Storage Technology	

Such a large power demand cannot be supported by the transmission line infrastructure that is currently in place. Currently, there are two options: either invest in a transmission line to boost capacity, or use distributed generation (DG) to meet consumer demand locally. DG has been defined differently by several authors from various points of view.

DG offers numerous benefits over centralized power generation, such as better voltage profile and less power system losses. To get the most benefits, the distribution system's planning stage must include the ideal DG placement and sizing. The system voltage profile may be impacted and power losses may increase as a result of suboptimal DG placement and sizing. Nonetheless, the best DG siting lowers transmission and distribution line losses, increasing the power system's overall capacity [2].

The multi-objective approach is utilized in the newly suggested method to get the best DG placement and sizing. The fitness function takes into account minimizing power losses and maximizing voltage stability by identifying the system's weakest link and voltage bus. Here, the multi-objective problem is solved using the Mountain Gazelle Optimizer (MGO). On the basis of improving the voltage profile, maximizing system load capacity, minimizing power system losses, and maximizing bus and line stability, this article also compares the suggested strategies with current practices. Additionally, the outcomes are verified on radial distribution networks of 33-bus and 85-bus, and they are thoroughly examined.

The issue of how lithium-ion batteries should operate optimally to raise the technical, financial, and environmental indices of both independent and grid-connected distribution networks is also addressed in this work. A general nonlinear programming model has been developed

as a result, which considers three objective functions: (i) the daily energy purchasing costs at the substation terminals, including the maintenance costs of renewable energy (photovoltaic) and energy storage technologies (batteries); (ii) the daily energy losses associated with energy transport; and (iii) the CO₂ emissions per day of operation associated with conventional generators. This is accomplished by combining all of the distributed network's functionalities and technological limitations with those of the devices that make up the network.

1.1. Literature review

A reliability-based optimal μ -PMU placement technique was presented by the authors in [3] for the effective observability enhancement of smart distribution grids in a variety of scenarios. The authors of [4] proposed an iterative convex approximation for the efficient day-ahead dispatch of photovoltaic sources in DC networks. Using MG's smart charging technique, the authors of [5] demonstrated multi-objective energy management with the charging impact of plug-in hybrid electric vehicles. The authors of [6] presented a sparse nonlinear optimization technique for optimizing power coordination in lithium-ion batteries, hence increasing the efficiency of the DC distribution network. The performance of grid-connected PV-EV charging stations can be enhanced by real-time dynamic power management combined with model predictive control, as the authors of [7] showed. The authors of [8] presented a distributed secondary consensus fault tolerant control method for managing power sharing and restoring voltage and frequency in multi-agent MGs. A authors of [9] introduced decarbonization to Mexico by growing the network of EV charging stations. The authors

of [10] presented a Deep Neural Network (DNN) method for optimizing electric car driving range prediction. In [11], authors presented a smart electricity market for a decarbonized MG's system. The authors examined a range of hybrid vehicle concepts that use biofuels and low temperature combustion as power sources in [12]. Based on optimal demand side management, the authors of [13] presented a novel approach to energy optimization in smart urban buildings. To maximize the enrichment of cobalt and lithium from spent lithium-ion polymer batteries, the authors of [14] recommended adjusting the high-temperature thermal pre-treatment parameters. An enhanced wombat optimization technique for multi-objective optimal power flow in integrated systems combining renewable energy and electric vehicles was presented by the authors in [15]. A novel approach to lowering carbon emissions was put forth by the authors of [16] using artificial intelligence and multi-renewable energy sources. The authors of [17] examined hybrid energy storage devices for electric vehicles that combine batteries and supercapacitors. A solution to the capacitor placement issue in radial distribution networks was put out by the authors in [18]. The authors of [19] presented a novel method for producing MPPT for SCADA based on photovoltaic systems. In [20], authors presented the fast crisscross sine cosine approach for optimal placement in power systems based on uncertain wind integrated situations. The ideal layout and positioning of a combined trench and submerged breakwater system for Aceh's coastline were suggested by the authors in [21]. Using mixed-integer-linear programming, the authors of [22] introduced a new communication platform for smart EMS. By employing the ZOA technique to allocate different DG types, the authors in [23] successfully decreased power losses. Authors of reference [24], introduced a bi-level programming approach for identifying and charging EV stations in distribution networks.

The authors of [25] used an enhanced butterfly optimization technique to provide a novel economic dispatch in the stand-alone system. A mixed-integer second-order cone model for the ideal placement and dimensions of dynamic reactive power compensators in distribution grids was put forth by the authors in [26]. A multi-objective augmented cockroach swarm algorithm technique for home energy management systems was presented by the authors in [27]. The authors of [28] presented hyperparameter optimization for estimating the state of distribution systems based on deep neural networks. The authors of [29] developed the GNDO technique to optimize distribution and solar static compensator planning in medium-voltage networks. A new cooperative controller for intelligent hybrid AC/DC MG's inverters was presented by the authors in [30]. The authors of [31] presented a low-voltage distribution network for dynamic voltage management based on renewable energy. The authors of [32] used PV-STATCOM and metaheuristic optimization to dynamically balance active and reactive power in distribution networks. A novel robust control technique for parallel-operated inverters in green energy applications was presented by the authors in [33]. A new deep learning architecture for figuring out the topology of distribution systems with missing PMU measurements was presented by the authors in [34]. Using the internet of energy, the authors of [35] presented a new real-time electricity scheduling system for residential energy management. A groundbreaking decentralized MG's control approach was presented by the authors of [36] in the context of the internet of energy. The authors of [37] proposed a stochastic risk avoidance-based optimal power system operating approach. The authors of [38] presented coalition game theory for intelligent MG's consensus-based demand management techniques. Authors of [39] investigated minigrids based on DC and AC to see whether minigrid would be more cost-effective for electrifying remote developing regions. In [40], authors investigated the efficiency of electrical networks that use both AC and DC operation methods. The authors of [41] presented a new, reliable smart energy management and demand reduction solution for internet of energy-based smart homes. The authors of [42] described an energy management system that uses an antlion optimizer to ensure that PV generators in distribution systems operate as efficiently as

feasible. The authors of [43] described how to improve the technical, economic, and environmental aspects of PV sources in DC networks by using a matrix hourly power flow and the vortex search method. The authors of [44] presented a novel optimization technique for an Internet of Things-based demand-side management system for homes. In combination with a DC MG, the authors of [45] showed decentralized primary control of an off-grid PV-battery system. The authors of [46] demonstrated the effective integration of solar PV systems into the smart grid using DC-grid. The authors of [47] introduced a weighted-based iterative convex solution methodology for multi-objective PV plant dispatch in monopolar DC grids. In [48], the authors presented a novel solution to day-ahead scheduling issues using the Internet of Things-based bald eagle search optimization method. An MG's-based stochastic optimal scheduling of distributed energy resources with electric vehicles that considers electricity pricing was proposed by the authors of [49]. The authors of [50] described creative methods for integrating renewable energy sources into electrical networks. The authors of [51] presented a brand-new distributed demand side management system enabled by the internet of things. A strong optimization framework for cchp customers' energy management with integrated demand response in the electrical market was described by the authors in [52]. The authors of [53] proposed multi-objective battery cooperation in distribution networks to reduce energy losses and CO₂ emissions at the same time. When water pumping motors were first introduced, the authors of [54] suggested utilizing superconducting magnetic energy storage to lessen voltage sag in a distribution system. The authors of [55] proposed a PHEVS charging technique that maximizes the use of renewable energy sources in MG's. The ideal distribution plan for battery energy storage devices was proposed by the authors of [56] in order to increase system reliability and voltage and frequency stability in weak grids.

1.2. Research gaps

From the literature, there are limitations and research gaps as follows;

- In many of the above studies, the authors did not use smart charging scheme for PHEVs.
- In many of the above studies, the authors did not deals with the problem regarding the optimal operation of lithium-ion batteries to improve the economic, technical, and environmental indices of standalone and grid-connected distribution networks.
- The authors did not employ a metaheuristic technique (such as Mountain Gazelle Optimizer (MGO), Improved Beluga Whale Optimization (IBWO), Arithmetic Optimization Algorithm (AOA), etc.) to determine the ideal size and location of the distributed generators in many systems, such as [29] and [53].

1.3. Contribution and paper structure

The main contributions of this paper are shortened as follows:

- In order to lessen the MG's reliance on the main grid by reducing the interconnection power flow in the grid, a power management scheme for dynamic charging of PHEVs in an MG is proposed in this study. The energy demand on the grid will be decreased under such a strategy since the charging power is locally produced in a "green" way using RERs. Additionally, the PHEV battery reduces the adverse effects of extensive RER integration in the distribution network by acting as an energy storage system for the RERs. Additionally, this study minimizes MG's reliance on the main grid by increasing RER generation to charge PHEVs while lowering energy consumption from the main grid.
- This work deals with the problem regarding the optimal operation of lithium-ion batteries to improve the economic, technical, and

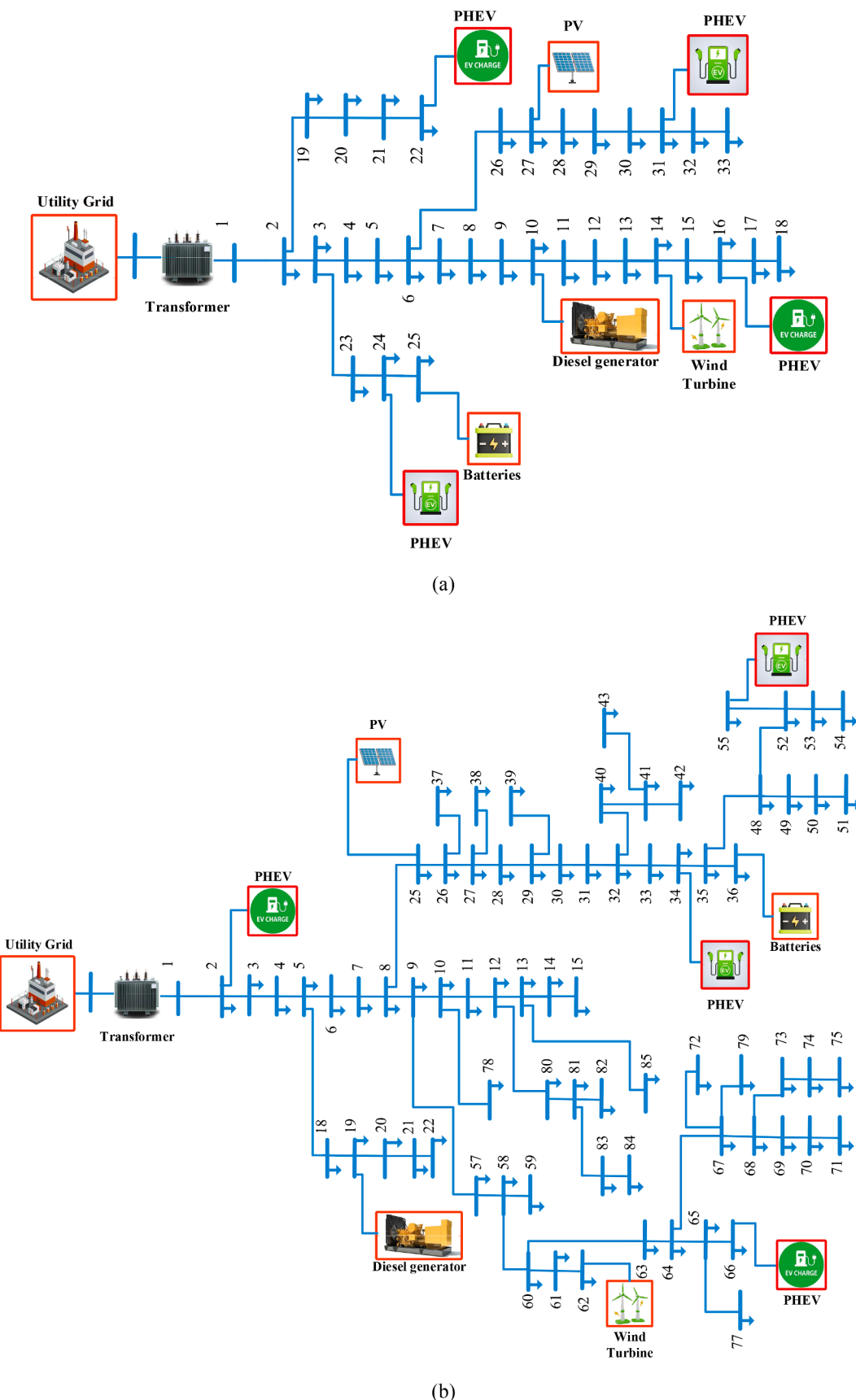


Fig. 1. Proposed IEEE bus distributed networks a) IEEE-33 bus, b) IEEE-85 bus.

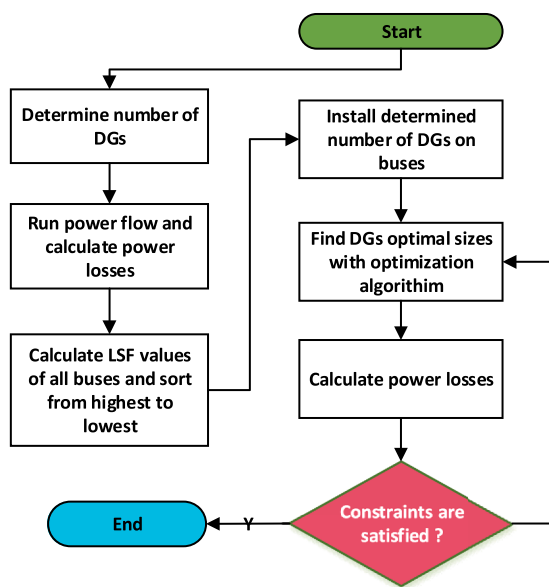


Fig. 2. The flowchart that shows where DGs should be placed.

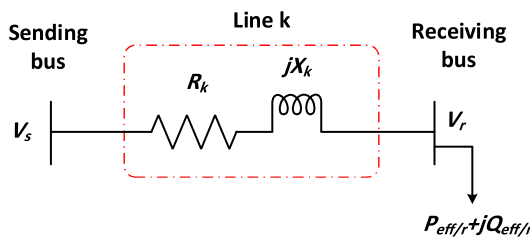


Fig. 3. Two-bus power distribution system.

environmental indices of standalone and grid-connected distribution networks.

- This paper offers a thorough explanation of the primary technical, financial, and environmental factors involved in the functioning of dispersed networks using the suggested mathematical framework. All of the limitations related to running distributed networks are included in this approach.
- The proposed methodology allows grid operators and researchers to obtain the best (optimal) solution at each execution.
- Mount Gazelle Optimizer (MGO) has been used to successfully determine each DG's capacity and placement while reducing overall power losses and voltage variance.
- The suggested algorithm has been applied to the IEEE 33-bus system in a number of scenarios, and the outcomes are contrasted with those of other well-known optimization techniques, including the Improved Beluga Whale Optimization (IBWO), and the Arithmetic Optimization Algorithm (AOA).

The remainder of paper is structured as follows: **Section 2** introduces suggested system configuration; **Section 3** describes methodology; **Section 4** shows the best location for the DGs; **Section 5** displays the enhanced beluga whale optimization algorithm; **Section 6** represents the mountain gazelle optimizer; **Section 7** shows the system modeling, results, and discussion; and **Section 8** wraps up the paper.

2. Proposed system configuration

A modified IEEE-33 and IEEE-85 node distributed network constructed on a grid-connected MG is illustrate in **Fig. 1**. The proposed

system consists of diesel generators, wind turbines, photovoltaics, storage units, and PHEVs.

2.1. Photovoltaics

Another emission-free green energy alternative is to install solar photovoltaic cells. Despite its advantages, PV power generation is limited by erratic intermittent characteristics. The temperature of the cell's module and the amount of sunlight determine how much electricity is generated by the solar output. The complete PV power production is represented mathematically by Eqs. (1) and (2), respectively, taking into account each parameter description from Ref. [57,58].

$$\mathcal{P}_{\text{pv}} = \mathcal{P}_{\text{src}} \frac{I_{\text{rad}}}{1000} (1 + \sigma(T_c - 25)) \quad (1)$$

$$T_c = T_a + \frac{I_{\text{rad}}}{800} (T_n - 20) \quad (2)$$

Where \mathcal{P}_{pv} is output power of photovoltaics, T_c is Temperature, I_{rad} is Solar irradiance

2.2. Battery modeling

This is how the battery is modeled [59,60]:

$$E_B(t) = E_B(t-1) + [P_B^{\text{dis}}(t) / \eta_{\text{dis}} - P_B^{\text{ch}}(t) \times \eta_{\text{ch}}] \quad \forall t, B \quad (3)$$

$$E_B^{\min} \leq E_B(t) \leq E_B^{\max} \quad \forall t, B \quad (4)$$

$$P_B^{\text{dis}}(t) / \eta_{\text{dis}} \leq P_B^{\max} \times \mu_B(t) \quad \forall t, B \quad (5)$$

$$P_B^{\text{ch}}(t) \times \eta_{\text{ch}} \leq P_B^{\max} \times (1 - \mu_B(t)) \quad \forall t, B \quad (6)$$

Eq. (3) defines battery's energy when charging and discharging, while Eq. (4) establishes the battery's maximum energy capacity. The discharge and charge power at any particular moment are reflected in Eqs. (5) and (6).

2.3. Plug-in electric vehicles (PEVs)

PEVs can be essential to achieving power balance in energy system because they are movable energy storage and provider units. Strategic use of PEVs as mobile energy storage/provider units can help prevent power imbalances that may result from changes in the supply and demand for electricity. The dynamic capabilities of PEVs can reduce emissions, maximize the utilization of renewable energy sources, and enhance energy system's stability and dependability. Dynamic model of PEVs in terms of SoC at time $(k+1)$ is found using the formula below [61]:

$$\text{SoC}_i^{\text{PEV}}(k+1) = \text{SoC}_i^{\text{PEV}}(k) + \frac{\Delta t}{\text{Cap}_{\text{ref}}^{\text{PEV}}} \left(\eta^{\text{ch}} \alpha_{\text{PEV}^{\text{ch}}}(k) P_{\text{PEV}_t}^{\text{ch}}(k) - \frac{\alpha_{\text{PEV}}^{\text{dis}}(k) P_{\text{PEV}}^t(k)}{\eta^{\text{dis}}} \right) \quad (7)$$

$$40\% \leq \text{SoC}_i^{\text{PEV}}(k) \leq 90\% \quad (8)$$

$$0 \leq P_{\text{PEV}_t}^{\text{ch}}(k) \leq \alpha_{\text{pev}}^{\text{ch}}(k) \bar{P}_{\text{PEV}_t}^{\text{ch}} \quad (9)$$

$$0 \leq P_{\text{PEV}_t}^{\text{dis}}(k) \leq \alpha_{\text{pev}}^{\text{dis}}(k) \bar{P}_{\text{PEV}_t}^{\text{dis}} \quad (10)$$

$$\alpha_{\text{pev}}^{\text{dis}}(k) + \alpha_{\text{pev}}^{\text{ch}}(k) \leq 1 \quad (11)$$

Eq. (7) constrains both upper and lower bounds of SoC. Constraints (9)–(10) limit charging and discharging powers. On the other hand, constraint (11) guarantees that charging and discharging cannot occur

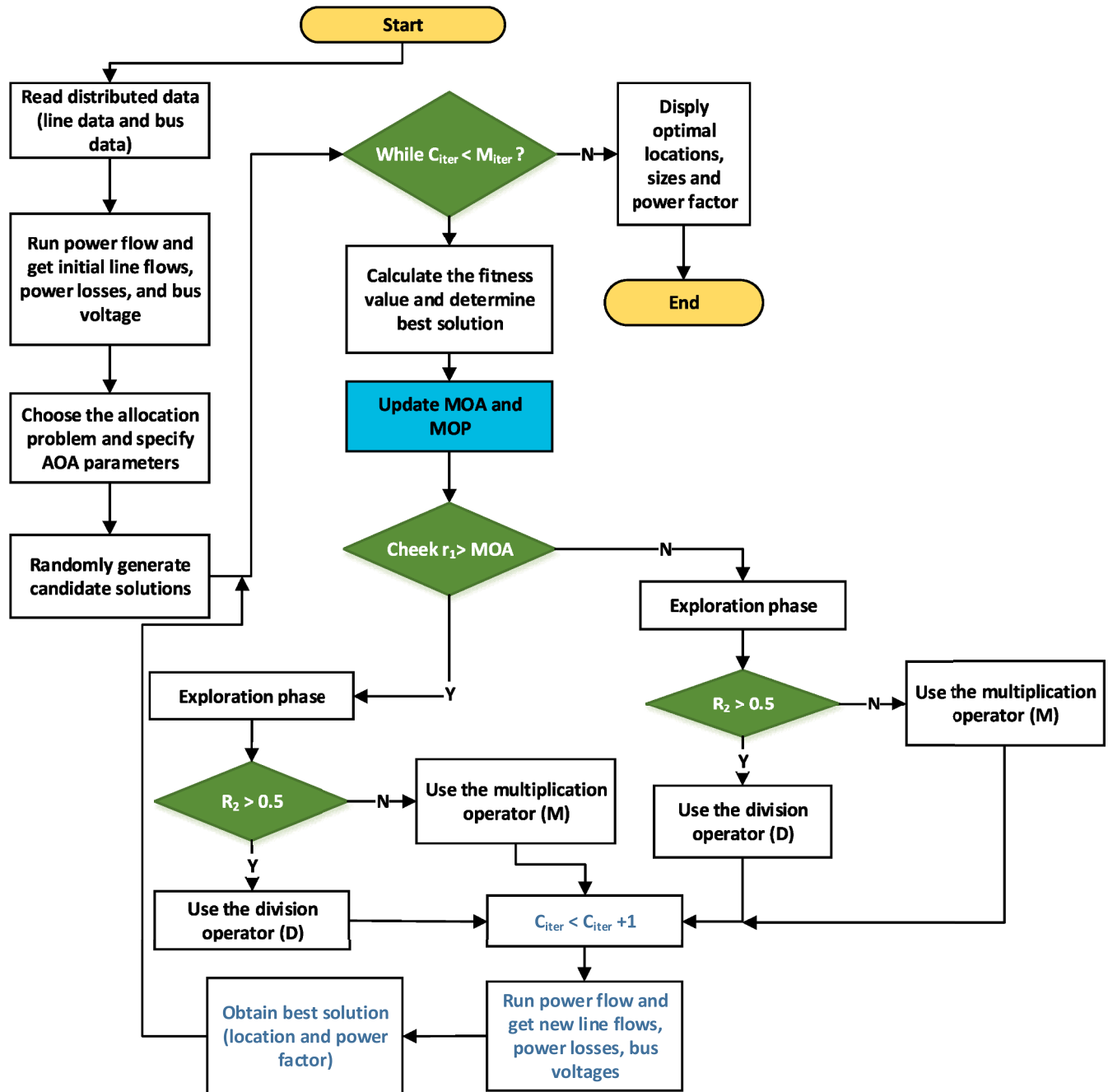


Fig. 4. AOA flowchart.

simultaneously. SoC and power pricing have a big impact on PEV consumers' decisions about charging and discharging their vehicles. These elements are essential to PEV owners' operational and financial concerns since they enable them to optimize their charging and discharging practices in accordance with grid conditions and economical energy management. Utilizing normal probability density function (Normal PDF), PEVs can be classified as either power producers or power consumers based on their SoC.

This classification is based on how much energy is stored in their batteries at any one moment k . PEVs with higher SoCs are frequently thought of as power providers, capable of releasing energy back into the grid, whilst those with lower SoCs are typically categorized as power consumers that need grid recharging. Normal PDF is a helpful tool for evaluating and predicting distribution of SoC among PEVs and, consequently, influencing how they perform in energy system. PEV charging

β^{ch} and discharging β^{dis} SoC impact factors are explained as:

$$\beta^{ch} = \begin{cases} M, & SoC_i^{PEV} < \mu \\ 1, & \mu \leq SoC_i^{PEV} < \nu \\ L, & SoC_i^{PEV} \geq \nu \end{cases} \quad (12)$$

$$\beta^{dis} = \begin{cases} L, & S_o C_i^{PEV} < \mu' \\ 1, & \mu' \leq S_o C_i^{PEV} < \nu' \\ M, & S_o C_i^{PEV} \geq \nu' \end{cases} \quad (13)$$

When a bigger constant with values of 0.1 and 3 is indicated by L , and a smaller constant is represented by M . Parameters μ and ν have been set to 0.3 and 0.6, respectively, while parameters μ' and ν' have also been

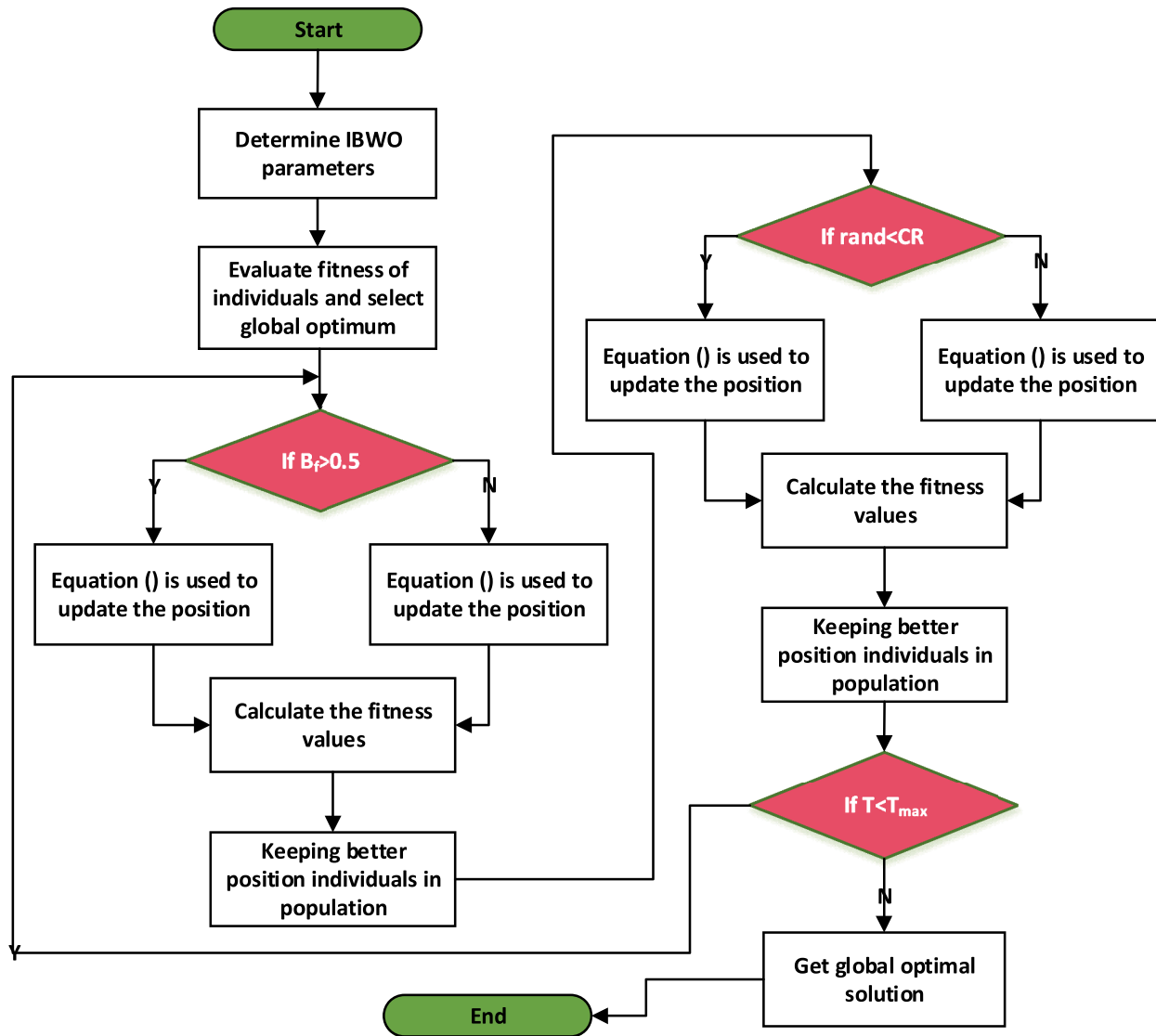


Fig. 5. Flowchart of IBWO.

assigned 0.3 and 0.6, respectively. The price of electricity, represented by the symbol λ_t , is the main factor affecting how PEVs charge and discharge.

3. Methodology

3.1. Problem formulation of smart charging scheme of PHEVs

3.1.1. Objective function

Suggested power management algorithm is formulated and provided in this section. It is recommended that PHEVs be charged dynamically, or with fluctuating charging power throughout the day, in order to lessen MG's reliance on upstream electrical grid and to get the majority of PHEV charging load from RERs/DER units. The energy that is taken from or added to the electric grid upstream is expressed as follows [62]:

$$P_{ex}(t) = P_{PHEV}(t) + P_{Load}(t) - P_{DER}(t) \quad (14)$$

where P_{DER} , P_{PHEV} , and $P_{Load}(t)$ stand for the MG's entire load, PHEV charging power, and combined output power of RERs and DERs. When $P_{ex} > 0$ in (14), power consumed by MG's load (i.e., load of ordinary and PHEVs) exceeds the DER units' output power, meaning that the upstream utility grid provides remaining energy required to charge MG's

load. On other hand, surplus electricity is supplied into the main grid when $P_{ex} < 0$. The entire amounts of energy that are drawn from upstream grid (E_{draw}) and fed to it (E_{fed}) in a day (24 h) are determined by:

When

$$P_{ex} < 0 : E_{fed} = \int_{t=0h}^{t=24h} P_{ex}(t)d(t) \quad (15)$$

When

$$P_{ex} > 0 : E_{draw} = \int_{t=0h}^{t=24h} P_{ex}(t)d(t) \quad (16)$$

$$E_{ex} = E_{draw} + E_{fed} \quad (17)$$

where E_{ex} is the total energy transferred to and from utility grid upstream. Minimizing total energy transferred with upstream grid (E_{ex}) is necessary to lessen MG's dependency on main grid and charge PHEVs while making the most use of RERs and DERs. A following method yields E_{DER} , the daily total output energy of DER units.

$$E_{DER} = \int_{t=1}^{t=24} P_{DER}(t)dt \quad (18)$$

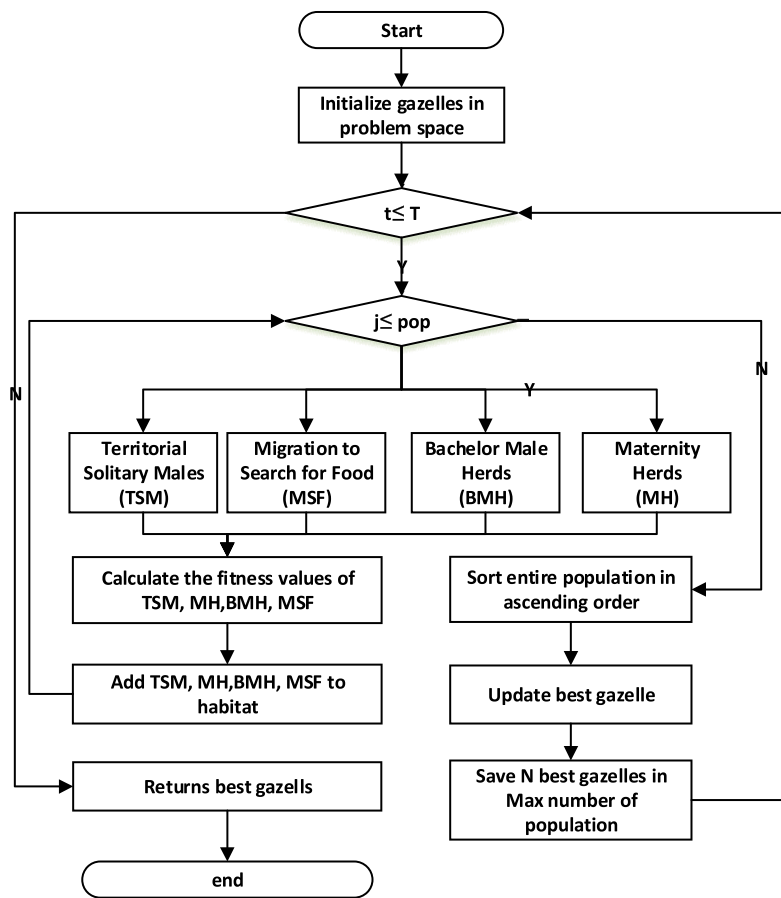


Fig. 6. MGO flowchart.

Table 1

Outcomes of IEEE 33-bus system's optimal DGs allocation, power loss, power factor, and average time.

Optimization type	Optimal location (Bus number)	Power loss (kW)	Loss Reduction (%)	Power factor	Average Time (s)
AOA	12	465.818 kW	6.83 %	0.88	21.85
	24				
	29				
IBWO	19	410.379 kW	17.92 %	0.92	27.61
	20				
	25				
MGO	9	386.521 kW	22.69 %	0.93	20.12
	13				
	27				

3.1.2. Constraints

The proposed design has to satisfy several limitations, such as those concerning voltage, power balance, and the generation of output power from RER/DER units Eqs. (19) and (20) provide power balance and voltage limitations, respectively.

$$P_{\text{RER}}(t) + P_{\text{grid}}(t) = P_{\text{PHEV}}(t) + P_{\text{Loss}}(t) + P_{\text{Load}}(t) \quad (19)$$

where $P_{\text{grid}}(t)$, $P_{\text{Load}}(t)$ and $P_{\text{Loss}}(t)$ represent upstream utility grid's output power, overall load, and MG's losses, respectively.

$$V_n^{\min} \leq V_{n,t} \leq V_n^{\max} \quad \forall n \in N, \forall t \in T \quad (20)$$

where V_n^{\max} , or 1.05 pu, is the highest voltage limit and V_n^{\min} , or 0.95 pu,

is the minimum voltage limit. N is number of buses in MG, and $V_{n,t}$ is voltage at bus n . Furthermore, constraints Eqs. (21) and (22) respectively express the DER units' active and reactive power restrictions.

$$P_{\text{DER}_i}^{\min} \leq P_{\text{DER}_i,t} \leq P_{\text{DER}_i}^{\max} \quad i = 1, 2, 3, \forall t \in T \quad (21)$$

$$Q_{\text{DER}_i}^{\min} \leq Q_{\text{DER}_i,t} \leq Q_{\text{DER}_i}^{\max} \quad i = 1, 2, 3, \forall t \in T \quad (22)$$

$P_{\text{DER}_i}^{\max}$ and $P_{\text{DER}_i}^{\min}$, respectively, represent upper and lower bounds on DER active power. $Q_{\text{DER}_i}^{\max}$ and $Q_{\text{DER}_i}^{\min}$ represent upper and lower bounds on DER reactive power, respectively. Furthermore, it's best to maintain output power of WT, PV array, and diesel generator within their maximum ranges.

$$0 \leq P_{\text{Diesel},t} \leq P_{\text{Diesel}}^{\max} \quad \forall t \in T \quad (23)$$

$$0 \leq P_{\text{WT},t} \leq P_{\text{WT}}^{\max} \quad \forall t \in T \quad (24)$$

$$0 \leq P_{\text{pv},t} \leq P_{\text{pv}}^{\max} \quad \forall t \in T \quad (25)$$

where P_{Diesel}^{\max} , P_{WT}^{\max} , and P_{pv}^{\max} represent the diesel generator's, WT's, and PV array's respective maximum output limitations.

4. Optimum location of the DGs

Determining where to locate DG systems is now one of most crucial steps in guaranteeing that consumers receive the power produced by DGs reliably and effectively. Because of this, it's essential to manage power flow, keep an eye on and regulate the amount of power generated by DGs, maintain system resilience, and keep supply and demand in check. DGs owners typically choose the best site for their facilities based

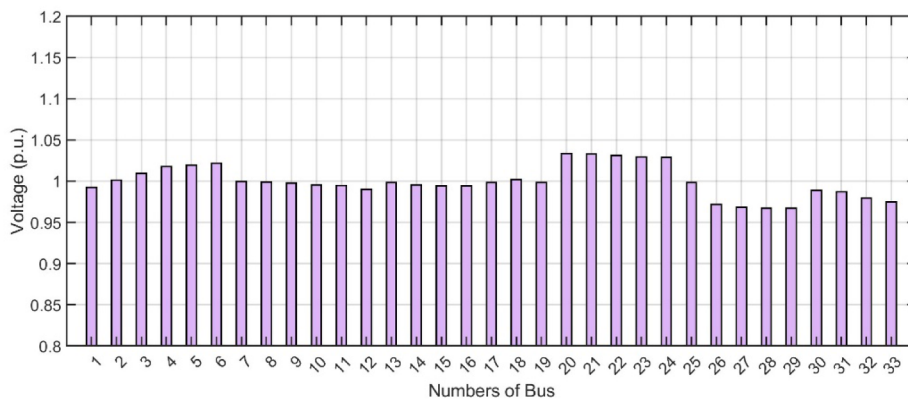


Fig. 7. voltage profiles for the various PHEV tiers.

on the highest profit possible, disregarding the previously listed factors. A distribution business (DISCO) that distributes electricity under license finds DG to satisfy customer demand, optimize profit, and develop best network investment plan. Although a distribution system operator (DSO) is primarily responsible for monitoring and developing a distribution system, the words DSO and DISCO are sometimes used interchangeably. In certain situations, DSO or DISCO may operate independently. A group called the Independent Distribution System Operator, or IDSO, works to increase the effectiveness and openness of power distribution. Additionally, IDSO can be used to plan distribution systems and locate DGs in an optimal manner. This study makes the assumption that the IDSO determines the best places for DGs. However, keep in mind that there may be regional or national variations in the definitions of DISCO, DSO, and IDSO, and that they may not be applicable to all electrical distribution systems.

With Loss Sensitivity Factor (LSF), the best locations for DGs and/or CBs are preset. The distribution system's buses are initially ranked from largest to smallest based on their LSF ratings. The buses that rank highest on the list are then chosen as possible candidates for the best DG and/or CB locations. After installing DG and/or CB on the candidate buses, the optimization method minimizes biggest power losses to determine the bus's ideal location. Fig. 2 expresses how to determine the best position for DGs and/or CBs.

4.1. Loss sensitivity factor

An approach to determining a distribution system's line's active power losses is to take a look at a two-bus distribution system, such the one shown in Fig. 3.

$$P_{\text{loss}} = R_k \cdot I_k^2 = R_k \cdot \left(\frac{P_{\text{eff}/r}^2 + Q_{\text{eff}/r}^2}{|V_r|^2} \right) \quad (26)$$

where voltage magnitudes at transmitting and receiving buses are indicated by the variables V_s and V_r , respectively. Phase angles at transmitting and receiving buses are denoted by the symbols δ_s and δ_r , respectively. The symbols R_k and X_k stand for the lines' resistance and reactance, respectively. I_k is current flowing across the line, and $P_{\text{eff}/r}^2$ and $Q_{\text{eff}/r}^2$ are sums of effective active and reactive power at receiving bus, respectively. Eq. (26) uses first derivatives based on reactive power to produce the LSF provided by Eq. (27) [63].

$$\text{LSF} = \frac{\partial P_{\text{loss}}}{\partial Q_{\text{eff}/r}} = \frac{2 \cdot Q_{\text{eff}/r} \cdot R_k}{V_r^2} \quad (27)$$

4.2. Power factor and optimal capacity

DGs are typically believed to have a power factor of unity.

Nonetheless, converters can be used to change the power factors of DGs that are based on inverters. Therefore, DGs alone can provide the power system with both active and reactive power, negating the requirement for CBs. Above equations are used to estimate the ideal power factor of each DG. Within constraints, ideal power factor and capacity are iteratively calculated using the recommended optimization algorithm and power flow analysis. The flowchart in Fig. 4 that shows optimal placement of DGs and/or CBs.

5. Improved beluga whale optimization algorithm (IBWO)

5.1. Initialization strategy

A produced starting population of the BWO algorithm is not able to cover the full solution space since it uses a random population initialization process. The enhanced initialization technique combines the Tent mapping and Sobol sequencing. The Tent map produces a chaotic sequence with a better distribution and diversity than the Sobol sequence, which produces a very uniform point set in space. Initial position distribution of beluga whale population may be more uniform within constraint range and cover a larger spatial range by combining the advantages of the two starting techniques.

A suggested initialization technique may improve algorithm's exploration performance. This is an expression for the function of improving an initialization procedure [64].

$$x_{T+1} = \begin{cases} x_T/h & x_T \in [0, h] \\ (x_T - 1)/(h - 1)x_T \in (h, 1] & \end{cases} \quad (28)$$

where the boundary constant is denoted by h , and 0.5 is its value.

5.2. Weight of dynamic self-adaptive features

A dynamic feature that adapts Weight is used throughout the IBWO algorithm's development. As the number of repetitions grows, the weight value first rises and then falls. The algorithm's optimization speed is accelerated in the method's early phases because of the reduced weight. Global search is aided by the adaptive weight, which progressively grows in value as the number of iterations increases and reaches its maximum in the middle stage. In the next iteration, the adaptive weight value is decreased, the search range is established, the ideal solution is located within a specified range, and algorithm's late-stage convergence speed is accelerated. The weights' value rapidly decreases as a number of iterations increases, hastening algorithm's convergence to the best answer. The dynamic self-adaptive feature weight formula is as:

$$W = \begin{cases} 2e^{-4(T_{\max} - T)/T_{\max}} & T \leq T_{\max}/2 \\ 2e^{-4T/T_{\max}} & T > T_{\max}/2 \end{cases} \quad (29)$$

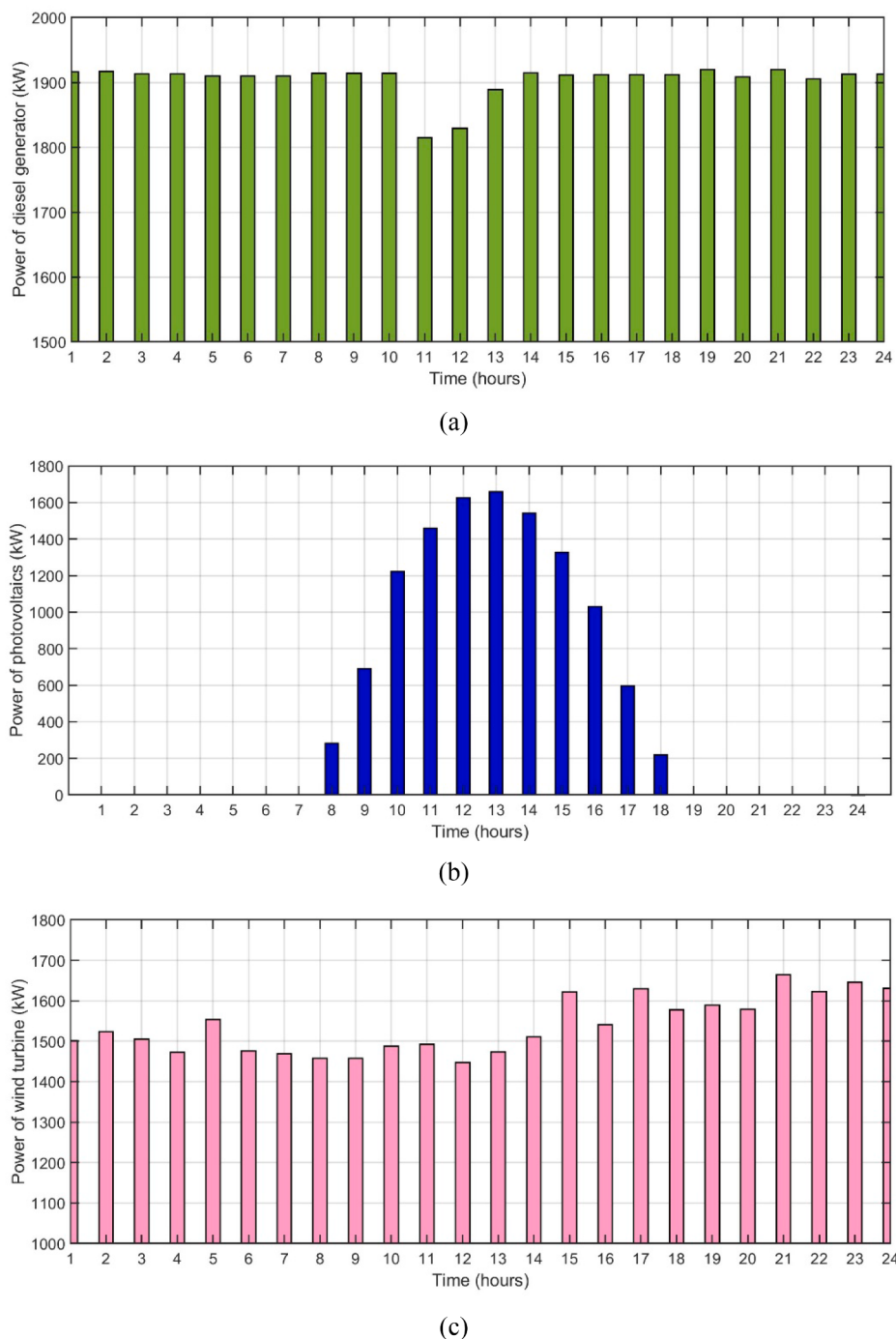


Fig. 8. Output active power of a) diesel generator, b) photovoltaic, c) wind turbine.

When beluga whales are developing, their positions are updated using the formula below: following the dynamic self-adaptive feature weight W's implementation.

$$X_i^{T+1} = r_3 X_{\text{best}}^T - W X_i^T + A \cdot L_F \cdot (X_r^T - X_i^T) \quad (30)$$

5.3. The ideal perturbation in the neighborhood

The problem of many smart algorithms finally leading to non-optimal results is not exclusive to the BWO method. To enhance convergence performance of the BWO method in a late iterations, interference is applied to current best solution as an iteration approaches a late stage. A few fresh ideas are created that are near the

current optimum answer. The equation for the new perturbation that this study suggests is as follows.

$$X_i^{T+1} = X_{\text{best}}^T + w_2 X_{\text{best}}^T \quad (31)$$

$$w_2 = \left[0.6 - 0.3 \left(\frac{T}{T} \right) \right] \cos \left(\frac{\pi}{2} \times r_5 \right) \quad (32)$$

where w_2 is a variable perturbation factor that will improve the procedure's accuracy of convergence by decreasing over the course of approach. Depending on degree of probability component CR, whale fall and the suggested ideal neighborhood perturbation alternate. In middle stages of the algorithm, the whale fall may enhance the number of

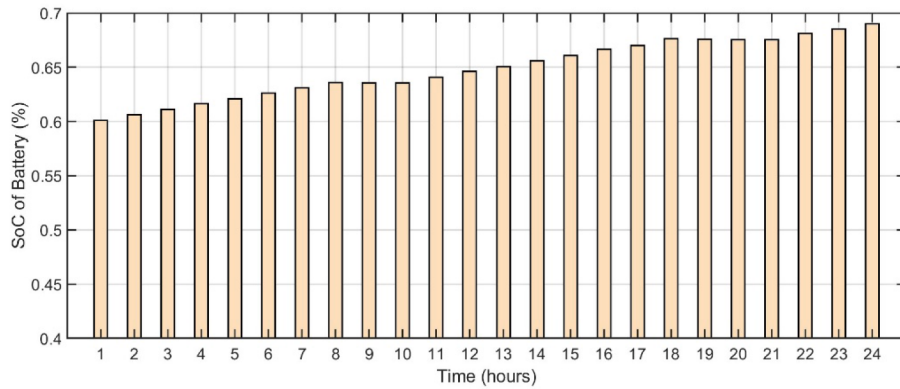


Fig. 9. SoCs of BESS by applying IEEE 33 Bus Network.

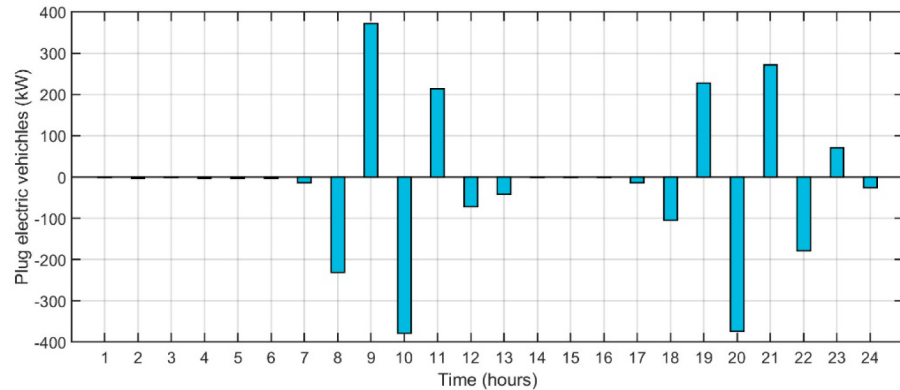


Fig. 10. PHEV load curves by applying IEEE 33 Bus Network.

Table 2
Information on the lines' resistive impact and the GCN's peak demand consumption.

Line	R _{1j} (0)	P _j (kW)	I (A)	Line	R _{1j} (0)	P _j (kW)	I (A)
1	0.0922	100	385	17	0.7320	90	20
2	0.4930	90	355	18	0.1640	90	40
3	0.3660	120	240	19	1.5042	90	25
4	0.3811	60	240	20	0.4095	90	20
5	0.8190	60	240	21	0.7089	90	20
6	0.1872	200	110	22	0.4512	90	85
7	1.7114	200	85	23	0.8980	420	85
8	1.0300	60	70	24	0.8960	420	40
9	1.0400	60	70	25	0.2030	60	125
10	0.1966	45	55	26	0.2842	60	110
11	0.3744	60	55	27	1.0590	60	110
12	1.4680	60	55	28	0.8042	120	110
13	0.5416	120	40	29	0.5075	200	95
14	0.5910	60	25	30	0.9744	150	55
15	0.7463	60	20	31	0.3105	210	30
16	1.2890	60	20	32	0.3410	60	20

potential solutions, but as it progresses, its impact decreases. With more iterations, there is a greater chance of ideal neighborhood disruptions, which can help the algorithm escape the local optimum.

This is how the revised formula for beluga whale location appears:

$$\begin{cases} X_i^{T+1} = r_5 X_i^T - r_6 X_r^T + r_7 X_s \text{rand} \geq CR \\ X_i^{T+1} = X_{\text{best}}^T + w_2 X_{\text{best}}^T \text{rand} < CR \end{cases} \quad (33)$$

where rand is a random variable with upper and lower bounds of 0 and 1 and CR is a probability factor. This is phrase:

$$CR = \cos\left(\frac{\pi}{2}\left(1 - \frac{T}{T_{\max}}\right)\right) \quad (34)$$

Fig. 5 displays the suggested IBWO algorithm's flowchart.

6. Mountain gazelle optimizer

Before delving deeply into the proposed approach and mathematical model, this part provides a quick overview of the primary inspiration for the MGO algorithm.

6.1. One species of gazelle is the Inspiration Mountain gazelle

Native to Arabian Peninsula and its surroundings, this species is extensively dispersed but has a low population density. Its surroundings are quite similar to those of Robinia tree species. A species lost portion of its distribution to the climatically acclimated Gazella bennettii as temperatures increased in the late Holocene. The mountain gazelle is fiercely protective of its territory. Their domain is separated from one another by a considerable distance. They divide into three groups: the region of lone males, young male herds, and mother-offspring herds. As the males mature into adulthood, the gazelles engage in regular combat. Compared to the conflict over female possession, the struggle between nearby males over the environment is more violent and dramatic. Immature men use their horns more for internal conflict than do older males or landowners [65].

6.2. Mathematical model

This article presents the optimization approach based on the social

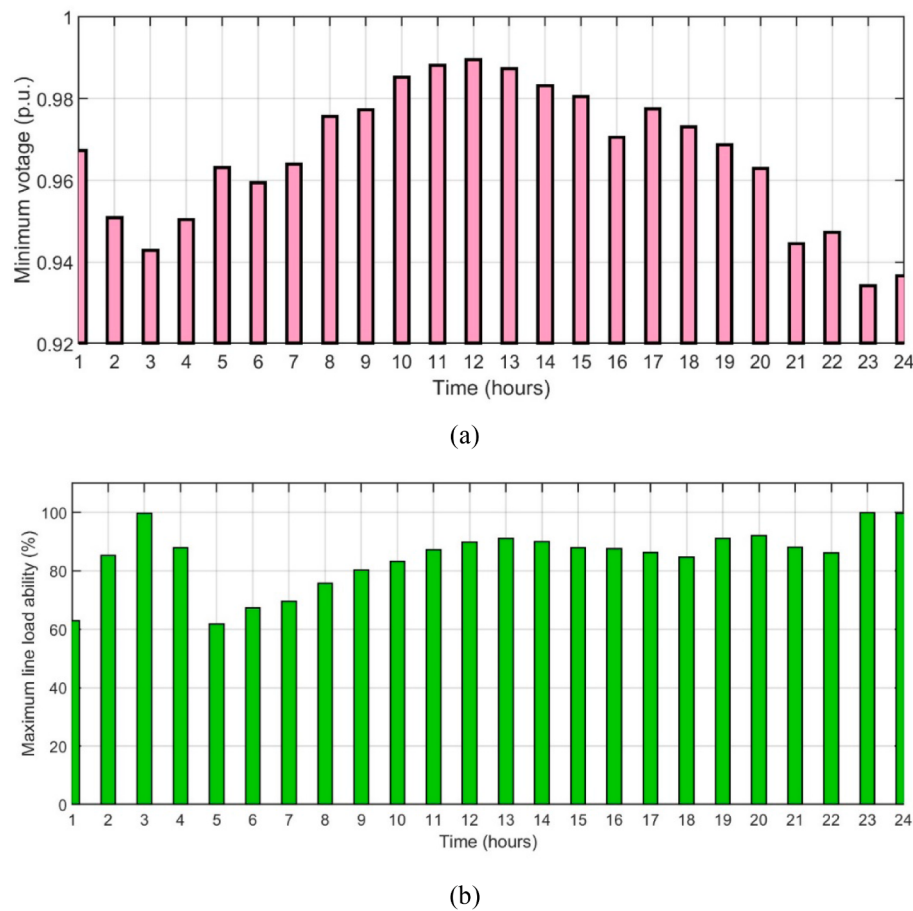


Fig. 11. (a) Minimum voltage characteristics, (b) maximum line load ability for the examined objective functions when the GCN is operating on a daily basis.

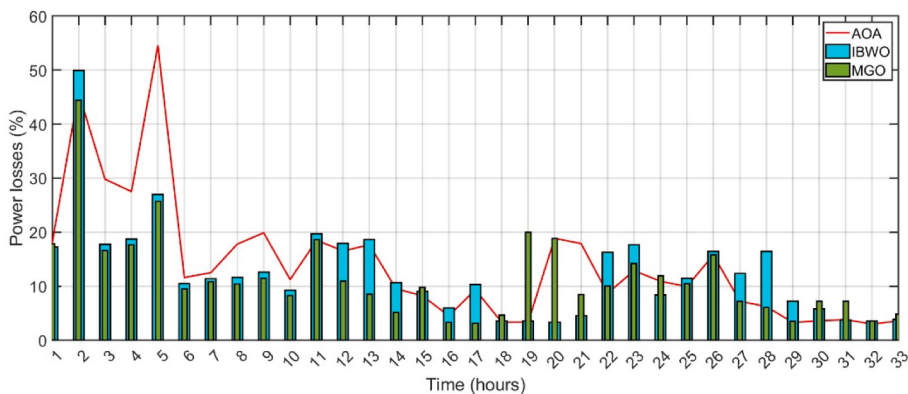


Fig. 12. Power loss at each bus of IEEE 33 bus distributed network using AOA in reference [63], using IBWO in reference [64], and MGO.

behaviors of mountain gazelles. An MGO algorithm mathematical model has been developed using fundamental ideas of social and group dynamics in mountain gazelle behavior. Four essential elements of mountain gazelle life are used in the MGO optimization technique: mobility in search of food, herds of maternity, herds of bachelor males, and lone, hostile males. Each gazelle (X_i) has the option to join maternity herds, bachelor male herds, or solitary, territorial males during the MGO algorithm's optimization phase. A baby gazelle can be found in any one of these three groups. Adult male gazelles that reside in herd areas are the best therapy for MGO in the globe. It is predicted that one-third of the search population in the entire population will be the least expensive option for mathematical modeling since the gazelles in the

male bachelor herds are still immature and not yet strong enough to procreate or seize control of the female gazelle.

Gazelle maternity herds are also contrasted with other choices that apply to the entire population. Strong gazelles with exceptional solutions are kept at end of each iteration. The sick and elderly gazelle population is eliminated, and the community as a whole is given access to more easily accessible alternative treatments. The following is a mathematical formulation and expression of the MGO's optimization operation mechanisms.

6.2.1. Territorial solitary males

Once adult and of a manageable size, male mountain gazelles form a

Table 3

The outcomes of IEEE 85-bus system's optimal DGs allocation, power loss, power factor, and average time

Optimization type	Optimal location (Bus number)	Power loss (Kw)	Loss Reduction (%)	Power factor	Average Time (s)
AOA	14	1973.702	1.31 %	0.729	29.3
	22	kW		0.912	
	35			0.889	
IBWO	38	1682.990	15.85 %	0.92	27.9
	49	kW		0.91	
	77			0.90	
MGO	40	1610.298	19.48 %	0.94	26.2
	48	kW		0.92	
	78			0.93	

single territory and become extremely territorial, leaving large gaps between territories. Male adult gazelles engage in combat over the territory or belongings of the female. Adult male territory has been predicted using Eq. (35).

$$TSM = \text{male}_{\text{gazelle}} - |(ri_1 \times BH - ri_2 \times X(t)) \times F| \times \text{Cof}_r \quad (35)$$

In Eq. (32) the location vector of ideal global solution is the male gazelle. A random numbers ri_1 and ri_2 are either 1 or 2. BH, or young male herd coefficient vector, is computed utilizing Eq. (36). Eq. (37), in addition, is used to calculate F. Eq. (38) is utilizing to calculate Cof_r, a randomly generated coefficient vector that is updated with each iteration and enhances the search capabilities.

$$BH = X_{ra} \times \lfloor r_1 \rfloor + M_{pr} \times \lceil r_2 \rceil, ra = \left\{ \left\lceil \frac{N}{3} \right\rceil \dots N \right\} \quad (36)$$

The random solution in interval of ra is described by X_{ra} in Eq. (36). Average number of randomly selected search agents ($\lceil \frac{N}{3} \rceil$) is denoted by M_{pr} . Additionally, N is total number of gazelles, while r_1 and r_2 are random integers between 0 and 1.

$$F = N_1(D) \times \exp \left(2 - \text{Iter} \times \left(\frac{2}{\text{MaxIter}} \right) \right) \quad (37)$$

In the issue's dimensions, N_1 is a random number selected from Eq. (37)'s standard distribution. Another name for the exponential function is exp. Iter indicates how many iterations are being performed at any given time, while MaxIter indicates how many iterations there are in total.

$$\text{Cof}_i = \begin{cases} (a + 1) + r_3, \\ a \times N_2(D), \\ r_4(D), \\ N_3(D) \times N_4(D)^2 \times \cos((r_4 \times 2) \times N_3(D)), \end{cases} \quad (38)$$

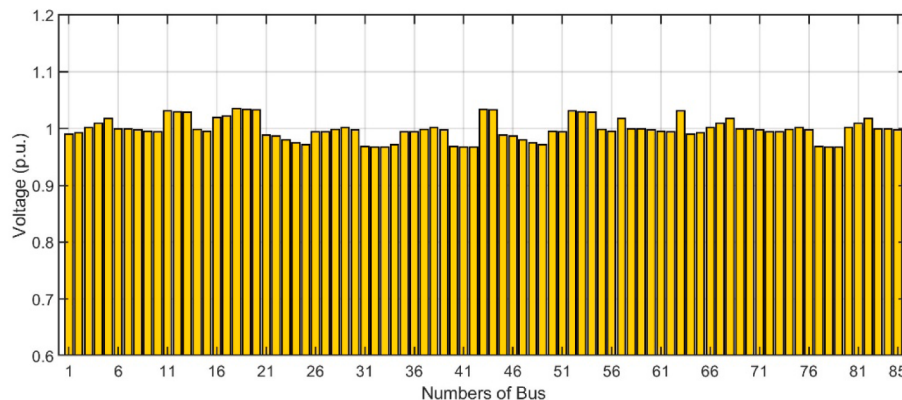


Fig. 13. voltage profiles for the various PHEV tiers by applying IEEE 85 Bus network.

The random values rand, r_3, r_4 are all between 0 and 1. The random numbers N_2, N_3 and N_4 are within the problem's dimensions and normal range. In the same way, r_4 is a random number between 0 and 1 in problem's dimensions. Finally, cos is a representation of Cosine function.

$$a = -1 + \text{Iter} \times \left(\frac{-1}{\text{MaxIter}} \right) \quad (39)$$

Finally, in Eq. (39), MaxIter indicates total number of iterations, while Iter indicates number of iterations that are currently occurring.

6.2.2. Maternity herds

Because these packs give birth to healthy male gazelles, maternity herds are essential to the life cycle of mountain gazelles. The birthing process and the young males' attempts to mate with females may also involve male gazelles. This behavior is formulated using Eq. (40).

$$MH = (BH + \text{Cof}_{1,r}) + (ri_3 \times \text{male}_{\text{gazelle}} - ri_4 \times X_{\text{rand}}) \times \text{Cof}_{1,r} \quad (40)$$

An impact factor of young males, denoted by vector BH in Eq. (40), is calculated using Eq. (36). The randomly selected coefficient vectors $\text{Cof}_{2,r}$ and $\text{Cof}_{3,r}$ are independently calculated using Eq. (39). ri_3 and ri_4 are composed of the integer and random numbers 1 or 2. Right now, "gazelle" is the finest worldwide solution because it is "male." Finally, vector position of a randomly selected gazelle from entire population is denoted via X_{rand} .

6.2.3. Bachelor male herds

Once they reach adulthood, male gazelles frequently create territories and take charge of female gazelles. At this stage, there could be a lot of fighting between the younger and older male gazelles to choose who gets to control the territory of the female gazelles. This gazelle action is mathematically described by Eq. (41).

$$BMH = (X(t) - D) + (ri_5 \times \text{male}_{\text{gazelle}} - ri_6 \times BH) \times \text{Cof}_r \quad (41)$$

The location of gazelle vector in current iteration is denoted by $X(t)$ in Eq. (41). Eq. (42) is utilized to calculate D. The randomly selected integers ri_5 and ri_6 are both 1 or 2. The optimum answer for the male gazelle vector is $\text{male}_{\text{gazelle}}$. Using above equation the impact factor of the young male herd, BH, is also determined. Utilizing Eq. (43) to compute the randomly chosen coefficient vector Cof_r.

$$D = (|X(t)| + |\text{male}_{\text{gazelle}}|) \times (2 \times r_6 - 1) \quad (42)$$

A position of gazelle vectors in current iteration is indicated by $X(t)$ and male gazelle, respectively, in Eq. (42), where best solution (adult male) is represented. r_6 is another arbitrary number between 0 and 1.

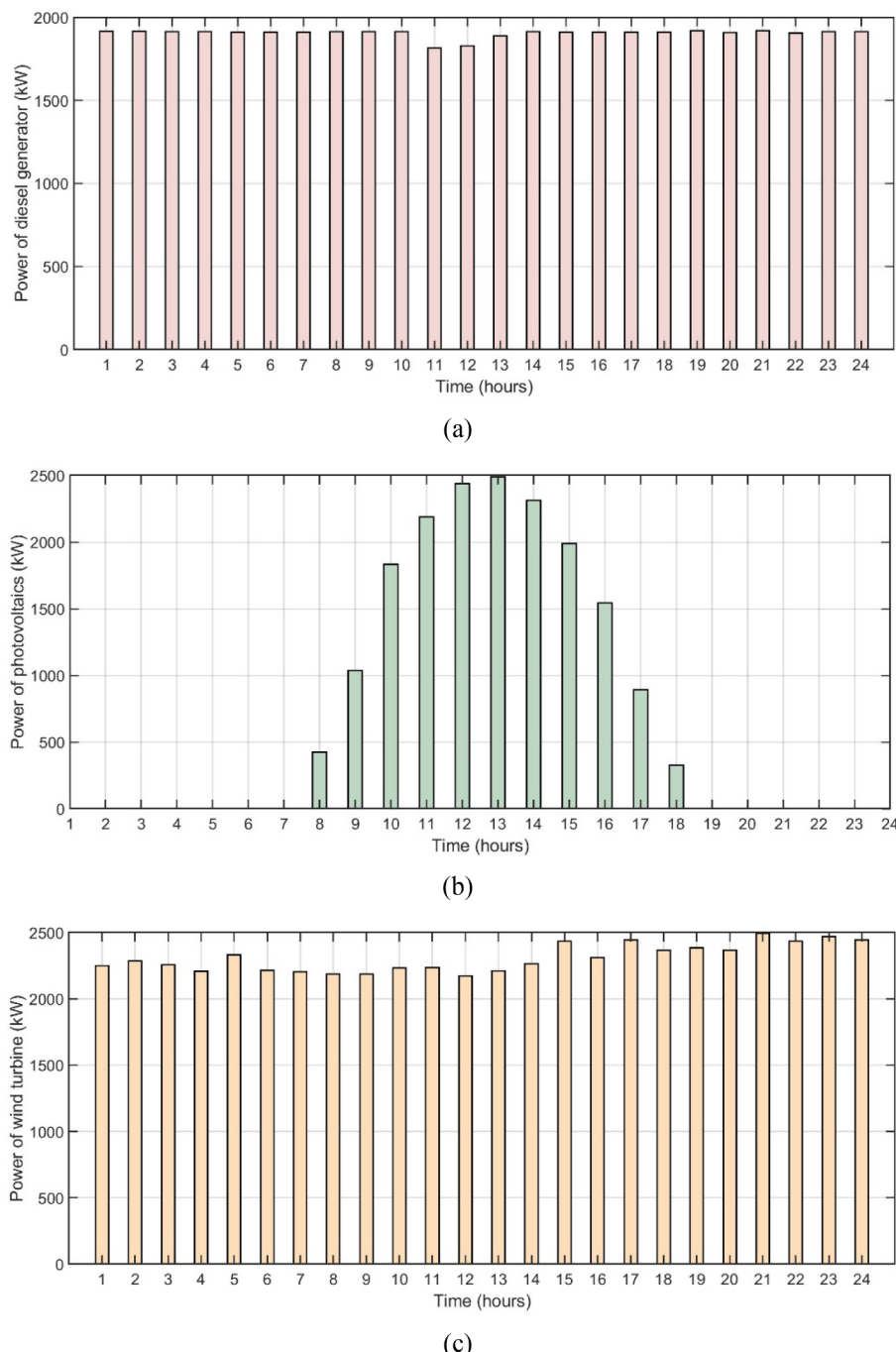


Fig. 14. Output active power of a) diesel generator, b) photovoltaic, and c) wind turbine by applying IEEE 85 Bus network.

6.2.4. Migration to search for food

Mountain gazelles travel great distances all year round in search of food. However, mountain gazelles are able to run fast and jump well. The mathematical formulation of this gazelle behavior is given by Eq. (43).

$$MSF = (ub - lb) \times r_7 + lb \quad (43)$$

An upper and lower boundaries of problem are represented by ub and lb , respectively, in Eq. (43). A number between 0 and 1 is selected at random to be r_7 . All gazelles are exposed to the four TSM, MH, BMH, and MSF procedures in order to generate new generations. A population grows via an era, with one replication for every generation. The best gazelles are those that are preserved across the population and offer high-quality, cost-effective solutions. Some gazelles are eliminated from

the population altogether because they are deemed old or feeble. Fig. 6 displays the MGO algorithm's flowchart.

7. Simulation outcomes

The several MATLAB-implemented optimization techniques for different bus systems, such as IEEE 33 Bus distributed network and IEEE 85 Bus distributed network, are evaluated in this part. A best way to distribute DG in a radial distribution system is to use a variety of techniques to reduce power loss and raise power factor. An updated MGO, AOA, and IBWO's performances are evaluated and compared. A major goal is to identify optimal optimization technique that minimizes the system's overall power loss, allowing for efficient operation. To find the optimum optimization algorithm, many scenarios are studied and

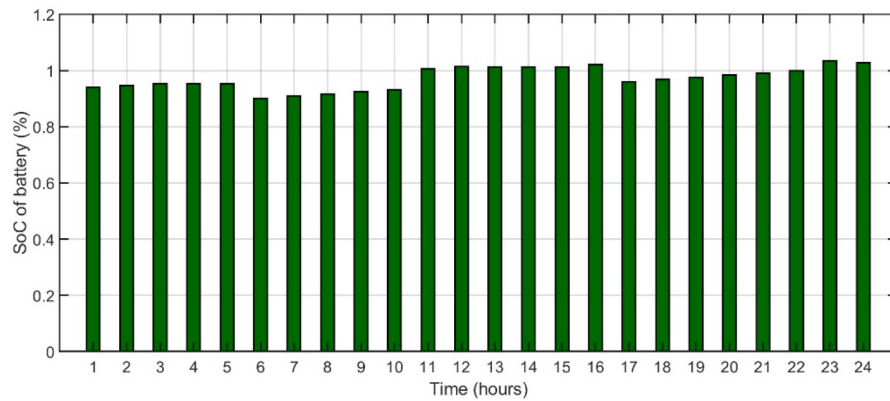


Fig. 15. SoCs of BESS by applying IEEE 85 bus system.

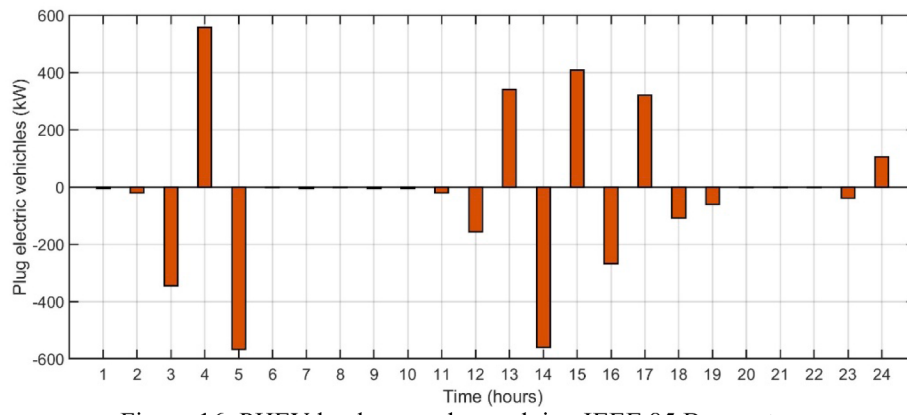


Fig. 16. PHEV load curves by applying IEEE 85 bus system.

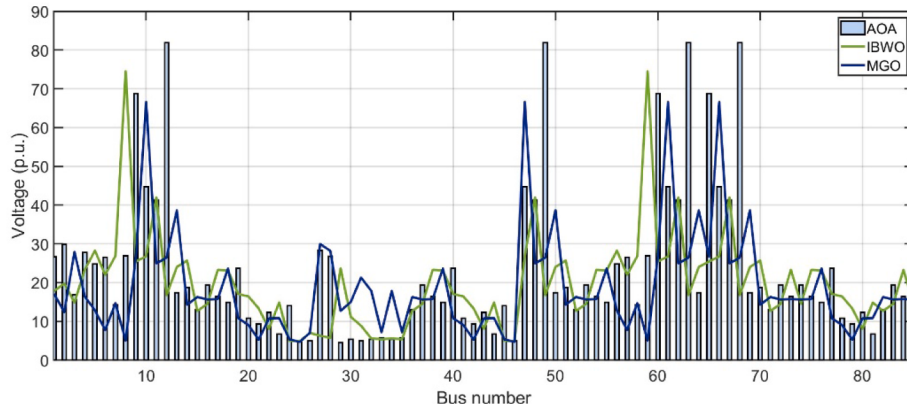


Fig. 17. Power loss at each bus of IEEE 85 bus distributed network using AOA in reference [63], using IBWO in reference [64] and MGO.

results are compared.

7.1. Discussion of results using IEEE 33 bus system

There are 33 buses and 32 lines in the IEEE 33-bus distribution network. Fig. 1 illustrate single line schematic as well as line and load statistics for system.

The IEEE 33-bus system's optimal DG allocation, power loss, power factor, and average time using AOA, IBWO, and MGO are shown in Table 1. When the outcomes from other optimization algorithms are compared, MGO yields the lowest power loss, best power factor correction and best average time to obtained results. When using the

AOA the Optimal location in buses 12, 24, and 29 bus, power loss was 465.818 kW, loss reduction was 6.83 (%), power factor is found 0.88, 0.89, 0.91 respectively, and average Time is found 21.85 second. But when using the IBWO the Optimal location in buses 19, 20, and 25 bus, power loss was 410.379 kW, loss reduction was 17.92 %, power factor is found 0.92, 0.93, 0.92 respectively, and average time is found 27.61 second. Whereas using the MGO the Optimal location in buses 9, 13, and 27 bus, power loss was 386.521 kW, loss reduction was 22.69 %, power factor is found 0.93, 0.95, 0.95 respectively, and average time is found 20.12 second.

The suggested power management plan, which bases charging of PHEVs on maximum utilization of RERs and DERs, is applied. In this

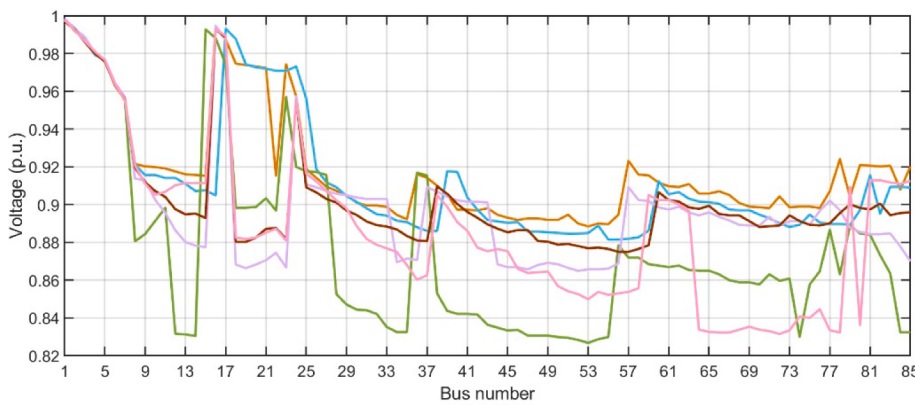


Fig. 18. Voltage profile of IEEE 85-bus practical system in various network configurations.

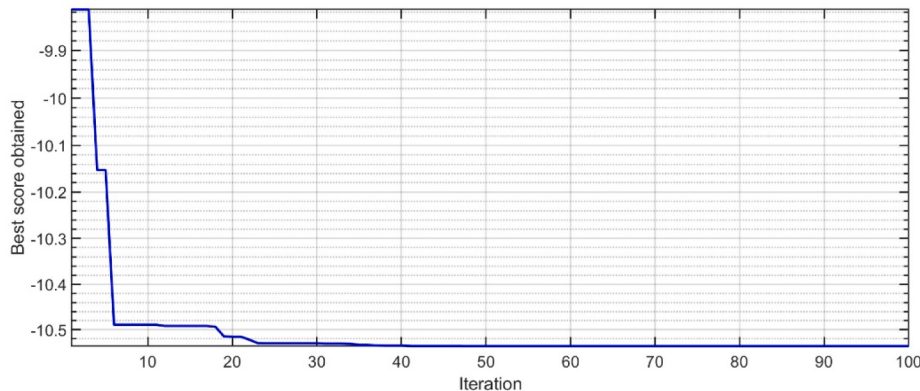


Fig. 19. the best score obtained vs iterations.

instance, DER units' output active power levels are estimated by optimization rather than predetermined. Fig. 7 illustrate voltage profiles for different PHEV levels. It should be noted that when the PHEVs are charged as recommended, the MG's voltage profile remains within a reasonable range. Furthermore, across the different PHEV penetration levels, the voltage profile stays rather stable. Fig. 8 shows the RER/DER units' active power levels during the course of a day at different PHEV levels. Put another way, the amount of electricity required to charge PHEVs. MG is less dependent on upstream utility grid to charge PHEVs since less energy is drawn from it when RER/DER units are used to generate power locally. Fig. 9 displays the BESS's SoCs for the different PHEV levels. The peak PHEV load hours coincide with the BESS discharge. Nonetheless, the quantity of energy that BESS supplies to grid during times of high PHEV load. A load curves for G2V and V2G modes of the PHEVs in each parking lot are displayed in Fig. 10. The PHEVs' base load is taken to be zero in this instance. Because of this, the load curves for PHEVs operating in V2G mode take on negative values, showing that a load is less than a base load, whereas load curves for PHEVs operating in G2V mode show that a load is more than a base load. Furthermore, when PHEV consumption increases, the MG can make use of the V2G mode. The Grid-Connected Network (GCN) with its RGTs and ESTs is depicted in Fig. 1, and Table 2 offers information on consumption peak demand, the lines' resistive effect, and their maximum capacities. Fig. 11 depicts the three ESTs in this system's working scheme. Similar to the SN, the SOC remains between 10 % and 90 % for every objective function, with beginning and ending points at 50 %. Fig. 12 shows the power loss of each bus for the two types of loads used to evaluate IEEE 33 bus system. When compared to the other options, study revealed that the modified MGO produced best results in terms of power loss and standard deviation.

7.2. Discussion of results using IEEE 85 bus system

There are 85 buses and 84 lines in the IEEE 85-bus network. Fig. 1 illustrate a single line schematic as well as a line and load statistics for the system. Table 3 displays the results of IEEE 85-bus system's optimal DGs allocation, power loss, power factor, and average time using AOA, IBWO and MGO. When the outcomes from other optimization algorithms are compared, MGO yields the lowest power loss, best power factor correction and best average time to obtained results. When using the AOA the Optimal location in buses 14, 22, and 35 bus, power loss was 1973.702 kW, loss reduction was 1.31 %, power factor is found 0.729, 0.912, 0.889 respectively, and average Time is found 29.3 second. But when using the IBWO the optimal location in buses 38, 49, and 77 bus, power loss was 1682.990 kW, loss reduction was 15.85 %, power factor is found 0.92, 0.91, 0.90 respectively, and average Time is found 27.9 second. Whereas using the MGO the optimal location in buses 40, 48, and 78 bus, power loss was 1610.298 kW, loss reduction was 19.48 %, power factor is found 0.94, 0.92, 0.93 respectively, and average time is found 26.2 second.

Fig. 13 shows voltage profiles for the various PHEV tiers by applying IEEE 85 Bus system. Fig. 14 illustrates the output active power of a) diesel generator, b) photovoltaic, and c) wind turbine by applying IEEE 85 Bus system. Fig. 15 illustrates SoCs of BESS by applying IEEE 85 Bus network. Fig. 16 illustrates PHEV load curves by applying IEEE 85 Bus network. Fig. 17 shows power loss at each bus of IEEE 85 bus distributed network using AOA in reference [63], using IBWO in reference [64] and MGO. Fig. 18 shows IEEE 85-bus practical system voltage profile under various network setups. Fig. 19 shows the best score obtained vs iterations.

8. Conclusions

In order to maximize energy supplied to the upstream grid and limit energy extracted from the MG, the proposed power management approach charged PHEVs with the highest usage of RERs/DERs in MGs. As a result, the MG was less dependent on the upstream grid. This study also took into account the stochastic nature of the PHEV charging profile and the output power from RERs. The comparisons and simulated scenarios that exploited the charging stations' V2G and G2V operating modes allow the PHEV batteries to function as BESSs for RERs and reduce the negative effects of the widespread integration of RERs into MGs. To assess efficacy of suggested power management and compare its outcomes with a previously published approach, two scenarios were developed for this study. Even in situations with a high degree of PHEV penetration, it has been demonstrated that the suggested power management strategy can reduce the amount of energy consumed from the upstream utility grid by charging PHEVs in accordance with the maximum usage of RERs and DERs. Furthermore, this study suggested using nonlinear optimization to schedule solar plants and lithium-ion batteries for grid-connected networks as efficiently as possible. The proposed method finds reductions of about 6.83 % in power losses using AOA, reductions of about 17.92 % in power losses using IBWO, reductions of about 22.69 % in power losses using MGO, when compared to the benchmark case in the IEEE 33-bus network, whereas the proposed method finds reductions of about 1.31 % in power losses using AOA, reductions of about 15.85 % in power losses using IBWO, reductions of about 19.48 % in power losses using MGO, when compared to the benchmark case in the IEEE 85-bus network. The study found that by determining where and how large to deploy DGs, the MGO algorithm was the most efficient way to minimize power loss.

Future studies could look into BESS's power capability, aging, and economics to get the most out of it. To improve system stability and dependability under weak grid settings, optimal BESS and DG operating strategies could be created. Additionally, in addition to BESS, other devices like electrolyze hydrogen (EH) will be taken into consideration in order to create a more efficient plan for improving system stability and dependability.

CRediT authorship contribution statement

Bilal Naji Alhasnawi: Writing – original draft, Formal analysis, Data curation, Conceptualization. **Marek Zanker:** Writing – review & editing, Funding acquisition. **Vladimír Bureš:** Writing – review & editing, Supervision, Funding acquisition.

Declaration of competing interest

The authors declare that they have no known competing financial interests or personal relationships that could have appeared to influence the work reported in this paper.

Acknowledgments

The research has been partially supported by the Faculty of Informatics and Management UHK excellence project "Methodological perspectives on modeling and simulation of hard and soft systems 2".

Data availability

No data was used for the research described in the article.

References

- [1] K. Kathiravan, P. Rajnarayanan, Application of AOA algorithm for optimal placement of electric vehicle charging station to minimize line losses, *Electric. Power Syst. Res.* 214 (2022) 108868, <https://doi.org/10.1016/j.epsr.2022.108868>.
- [2] M. Aman, G. Jasmon, A. Bakar, H. Mokhlis, A new approach for optimum DG placement and sizing based on voltage stability maximization and minimization of power losses, *Energy Convers. Manage.* 70 (2013) 202–210, <https://doi.org/10.1016/j.enconman.2013.02.015>.
- [3] A. Abdolah, N. Taghizadegan, M.R. Banaei, J. Salehi, A reliability-based optimal μ -PMU placement scheme for efficient observability enhancement of smart distribution grids under various contingencies, *IET Sci. Measur. Technol.* 15 (8) (2021) 663–680, <https://doi.org/10.1049/sm2.12067>.
- [4] O.D. Montoya, L. Fernando, J.C. Hernández, Efficient day-ahead dispatch of photovoltaic sources in monopolar DC networks via an iterative convex approximation, *Energies* 16 (3) (2022) 1105, <https://doi.org/10.3390/en16031105>.
- [5] A. Chakraborty, S. Ray, Multi-objective energy management using a smart charging technique of a microgrid with the charging impact of plug-in hybrid electric vehicles, *Sustain. Cities Society* 117 (2024) 105923, <https://doi.org/10.1016/j.scs.2024.105923>.
- [6] L.F. Grisales-Noreña, B. Cortes-Caicedo, O.D. Montoya, W. Gil-González, J. Muñoz, Enhancing DC distribution network efficiency through optimal power coordination in lithium-ion batteries: a sparse nonlinear optimization approach, *J. Energy Storage* 96 (2024) 112484, <https://doi.org/10.1016/j.est.2024.112484>.
- [7] A. Watil, H. Choja, Enhancing grid-connected PV-EV charging station performance through a real-time dynamic power management using model predictive control, *Results Eng.* 24 (2024) 103192, <https://doi.org/10.1016/j.rineng.2024.103192>.
- [8] B.N. Alhasnawi, B.H. Jasim, B.E. Sedhom, Distributed secondary consensus fault tolerant control method for voltage and frequency restoration and power sharing control in multi-agent microgrid, *Int. J. Electr. Power Energy Syst.* 133 (2021) 107251, <https://doi.org/10.1016/j.ijepes.2021.107251>.
- [9] F. Ruiz-Barajas, A. Ramírez-Nafarrete, E. Olivares-Benítez, Decarbonization in Mexico by extending the charging stations network for electric vehicles, *Results Eng.* 20 (2023) 101422, <https://doi.org/10.1016/j.rineng.2023.101422>.
- [10] S.A. Hasib, M.M. Gulzar, A. Shakoor, S. Habib, A.F. Murtaza, Optimizing electric vehicle driving range prediction using deep learning: A deep neural network (DNN) approach, *Results Eng.* 24 (2024) 103630, <https://doi.org/10.1016/j.rineng.2024.103630>.
- [11] B.N. Alhasnawi, M. Zanker, V. Bureš, A smart electricity markets for a decarbonized microgrid system, *Electr. Eng.* (2024), <https://doi.org/10.1007/s00202-024-02699-9>.
- [12] A. García, J. Monsalve-Serrano, Analysis of a series hybrid vehicle concept that combines low temperature combustion and biofuels as power source, *Results Eng.* 1 (2019) 100001, <https://doi.org/10.1016/j.rineng.2019.01.001>.
- [13] B. Naji Alhasnawi, B.H. Jasim, A. Naji Alhasnawi, F.F.K. Hussain, R.Z. Homod, H. A. Hasan, O. Ibrahim Khalaf, R. Abbassi, B. Bazooyar, M. Zanker, V. Bureš, B. E. Sedhom, A novel efficient energy optimization in smart urban buildings based on optimal demand side management, *Energy Strategy Rev.* 54 (2024) 101461, <https://doi.org/10.1016/j.esr.2024.101461>.
- [14] L. Gao, P. Afreh, A. Sidhoum, W. Zhang, Optimization of high-temperature thermal pretreatment conditions for maximum enrichment of lithium and cobalt from spent lithium-ion polymer batteries, *Results Eng.* 23 (2024) 102802, <https://doi.org/10.1016/j.rineng.2024.102802>.
- [15] K. Nagarajan, A. Rajagopalan, M. Bajaj, V. Raju, V. Blazek, Enhanced wombat optimization algorithm for multi-objective optimal power flow in renewable energy and electric vehicle integrated systems, *Results Eng.* 25 (2025) 103671, <https://doi.org/10.1016/j.rineng.2024.103671>.
- [16] B.N. Alhasnawi, S.M.M. Almutoki, F.F.K. Hussain, A. Harrison, B. Bazooyar, M. Zanker, V. Bureš, A new methodology for reducing carbon emissions using multi-renewable energy systems and artificial intelligence, *Sustain. Cities Society* 114 (2024) 105721, <https://doi.org/10.1016/j.scs.2024.105721>.
- [17] C.V.M. Gopi, R. Ramesh, Review of battery-supercapacitor hybrid energy storage systems for electric vehicles, *Results Eng.* 24 (2024) 103598, <https://doi.org/10.1016/j.rineng.2024.103598>.
- [18] M.A.E.S. Mohamed El-Saeed, A.F. Abdel-Gwaad, M.A.F Farahat, Solving the capacitor placement problem in radial distribution networks, *Results Eng.* 17 (2023) 100870, <https://doi.org/10.1016/j.rineng.2022.100870>.
- [19] B.N. Alhasnawi, B.H. Jasim, A.N. Alhasnawi, B.E. Sedhom, A.M. Jasim, A. Khalili, V. Bureš, A. Burgio, P. Siano, A novel approach to achieve MPPT for photovoltaic system based SCADA, *Energies* 15 (22) (2021) 8480, <https://doi.org/10.3390/en15228480>.
- [20] S.P. Agrawal, P. Jangir, L. Abualigah, S.B. Pandya, A. Parmar, A.E. Ezugwu, A. Smerat, The quick crisscross sine cosine algorithm for optimal FACTS placement in uncertain wind integrated scenario based power systems, *Results Eng.* (2024) 103703, <https://doi.org/10.1016/j.rineng.2024.103703>.
- [21] I. Magdalena, M.N.F. Dhiya, H. Rifatin, K.A. Sidarto, A. Kania, Optimal design and placement of a combined trench and submerged breakwater system on the coastal area of Aceh, *Results Eng.* 24 (2024) 102785, <https://doi.org/10.1016/j.rineng.2024.102785>.
- [22] B.N. Alhasnawi, B.H. Jasim, B.E. Sedhom, et al., A new communication platform for smart EMS using a mixed-integer-linear-programming, *Energy Syst.* (2023), <https://doi.org/10.1007/s12667-023-00591-2>.
- [23] A.A. Kandel, H. Kanaan, T. Mahmoud, B. Saad, Efficient reduction of power losses by allocating various DG types using the ZOA algorithm, *Results Eng.* 23 (2024) 102560, <https://doi.org/10.1016/j.rineng.2024.102560>.
- [24] R. Aazami, M.M. Badan, M. Shirkhani, A. Azizi, Bi-level programming model of location and charging electric vehicle stations in distribution networks, *Results Eng.* 24 (2024) 103657, <https://doi.org/10.1016/j.rineng.2024.103657>.

- [25] B.N. Alhasnawi, B.H. Jasim, V. Bureš, B.E. Sedhom, A.N. Alhasnawi, R. Abbassi, M. R.M. Alsemawai, P. Siano, J.M. Guerrero, A novel economic dispatch in the stand-alone system using improved butterfly optimization algorithm, *Energy Strategy Rev.* 49 (2023) 101135, <https://doi.org/10.1016/j.esr.2023.101135>.
- [26] W. Gil-González, O.D. Montoya, L.F. Grisales-Noreña, C.L. Trujillo, D.A. Giral-Ramírez, A mixed-integer second-order cone model for optimal siting and sizing of dynamic reactive power compensators in distribution grids, *Results Eng.* 15 (2022) 100475, <https://doi.org/10.1016/j.rineng.2022.100475>.
- [27] B.N. Alhasnawi, B.H. Jasim, A.M. Jasim, V. Bureš, A.N. Alhasnawi, R.Z. Homod, M. R. Alsemawai, R. Abbassi, B.E. Sedhom, A multi-objective improved cockroach swarm algorithm approach for apartment energy management systems, *Information* 14 (10) (2023) 521, <https://doi.org/10.3390/info14100521>.
- [28] G. Békési, L. Barancsuk, B. Hartmann, Deep neural network based distribution system state estimation using hyperparameter optimization, *Results Eng.* 24 (2024) 102908, <https://doi.org/10.1016/j.rineng.2024.102908>.
- [29] O.D. Montoya, W. Gil-González, L.F. Grisales-Noreña, Optimal planning of photovoltaic and distribution static compensators in medium-voltage networks via the GNDO approach, *Results Eng.* 23 (2024) 102764, <https://doi.org/10.1016/j.rineng.2024.102764>.
- [30] B.N. Alhasnawi, B.H. Jasim, W. Issa, M.D. Esteban, A novel cooperative controller for inverters of smart hybrid AC/DC microgrids, *Appl. Sci.*, 10 (17) (2019) 6120, <https://doi.org/10.3390/app10176120>.
- [31] C. Hou, C. Zhang, P. Wang, S. Liu, Renewable energy based low-voltage distribution network for dynamic voltage regulation, *Results Eng.* 21 (2024) 101701, <https://doi.org/10.1016/j.rineng.2023.101701>.
- [32] J.D. Combita-Murcia, C.A. Romero-Salcedo, O.D. Montoya, D.A. Giral-Ramírez, Dynamic compensation of active and reactive power in distribution systems through PV-STATCOM and metaheuristic optimization, *Results Eng.* 22 (2024) 102195, <https://doi.org/10.1016/j.rineng.2024.102195>.
- [33] B.N. Alhasnawi, B.H. Jasim, W. Issa, F. Blaabjerg, A new robust control strategy for parallel operated inverters in green energy applications, *Energies* 13 (13) (2019) 3480, <https://doi.org/10.3390/en13133480>.
- [34] Y. Raghuvamsi, K. Teeparthi, V. Kosana, A novel deep learning architecture for distribution system topology identification with missing PMU measurements, *Results Eng.* 15 (2022) 100543, <https://doi.org/10.1016/j.rineng.2022.100543>.
- [35] B.N. Alhasnawi, B.H. Jasim, P. Siano, J.M. Guerrero, A novel real-time electricity scheduling for home energy management system using the internet of energy, *Energies* 14 (11) (2020) 3191, <https://doi.org/10.3390/en14113191>.
- [36] B.N. Alhasnawi, B.H. Jasim, B.E. Sedhom, E. Hossain, J.M. Guerrero, A new decentralized control strategy of microgrids in the internet of energy paradigm, *Energies* 14 (8) (2020) 2183, <https://doi.org/10.3390/en14082183>.
- [37] X. Wu, Q. Ji, F. Liu, Q. Du, W. Xu, Optimal operation strategy of power system based on stochastic risk avoidance, *Results Eng.* 21 (2024) 101832, <https://doi.org/10.1016/j.rineng.2024.101832>.
- [38] B.N. Alhasnawi, B.H. Jasim, B.E. Sedhom, J.M. Guerrero, Consensus algorithm-based coalition game theory for demand management scheme in smart microgrid, *Sustain. Cities Society* 74 (2021) 103248, <https://doi.org/10.1016/j.scs.2021.103248>.
- [39] N.N. Opiyo, A comparison of DC- versus AC-based minigrids for cost-effective electrification of rural developing communities, *Energy Rep.* 5 (2019) 398–408, nov.
- [40] O.D. Montoya, F.M. Serra, C.H.D. Angelo, On the efficiency in electrical networks with AC and DC operation technologies: a comparative study at the distribution stage, *Electronics* 9 (9) (2020) 1352, aug.
- [41] B.N. Alhasnawi, B.H. Jasim, Z. Rahman, P. Siano, A novel robust smart energy management and demand reduction for smart homes based on internet of energy, *Sensors* 21 (14) (2020) 4756, <https://doi.org/10.3390/s21144756>.
- [42] B. Cortés-Caicedo, L.F. Grisales-Noreña, O.D. Montoya, M.A. Rodriguez-Cabal, J. A. Rosero, Energy management system for the optimal operation of pv generators in distribution systems using the antlion optimizer: A colombian urban and rural case study, *Sustainability* 14 (23) (2022) 16083.
- [43] L.F. Grisales-Noreña, A.A. Rosales-Muñoz, B. Cortés-Caicedo, O.D. Montoya, F. Andrade, Optimal operation of PV sources in DC grids for improving technical, economical, and environmental conditions by using vortex search algorithm and a matrix hourly power flow, *Mathematics* 11 (1) (2022) 93.
- [44] B.N. Alhasnawi, B.H. Jasim, R. Mansoor, A.N. Alhasnawi, A.S. A Rahman, H. H. Alhelou, J.M. Guerrero, A.M. Dakhil, P. Siano, A new Internet of Things based optimization scheme of residential demand side management system, *IET Renew. Power Gener.* 16 (10) (2022) 1992–2006, <https://doi.org/10.1049/rpg2.12466>.
- [45] R. Ranjan, A. Panchbhai, A. Kumar, Decentralized primary control of PV-battery system integrated with DC microgrid in off-grid mode, in: 2022 IEEE International Conference on Power Electronics, Smart Grid, and Renewable Energy (PESGRE), IEEE, 2022 jan.
- [46] S. Rauf, A. Wahab, M. Rizwan, S. Rasool, N. Khan, Application of Dc-grid for Efficient use of solar PV System in Smart Grid, *Procedia Comput. Sci.* 83 (2016) 902–906.
- [47] O.D. Montoya, L.F. Grisales-Noreña, D.A. Giral-Ramírez, Multi-objective dispatch of pv plants in monopolar dc grids using a weighted-based iterative convex solution methodology, *Energies* 16 (2) (2023) 976.
- [48] B.N. Alhasnawi, B.H. Jasim, P. Siano, H.H. Alhelou, A novel solution for day-ahead scheduling problems using the iot-based bald eagle search optimization algorithm, *Inventions* 7 (3) (2022) 48, <https://doi.org/10.3390/inventions7030048>.
- [49] T. Hai, A.K. Alazzawi, J. Mohamad Zain, H. Oikawa, A stochastic optimal scheduling of distributed energy resources with electric vehicles based on microgrid considering electricity price, *Sustain. Energy Technol. Assessm.* 55 (2023) 102879, Feb.
- [50] S. Islam, N.K. Roy, Renewables integration into power systems through intelligent techniques: implementation procedures, key features, and performance evaluation, *Energy Rep.* 9 (2023) 6063–6087, Dec.
- [51] B.N. Alhasnawi, B.H. Jasim, A new internet of things enabled trust distributed demand side management system, *Sustain. Energy Technol. Assessm.* 46 (2021) 101272, <https://doi.org/10.1016/j.seta.2021.101272>.
- [52] L. Chen, H. Tang, J. Wu, C. Li, Y. Wang, A robust optimization framework for energy management of cchp users with integrated demand response in electricity market, *Int. J. Electr. Power Energy Syst.* 141 (2022) 108181, Oct.
- [53] O.D. Montoya, L.F. Grisales-Noreña, W. Gil-González, Multi-objective battery coordination in distribution networks to simultaneously minimize co2 emissions and energy losses, *Sustainability* 16 (5) (2024) 199, Feb.
- [54] M. Hashem, M. Abdell-Salam, M. Nayel, M.T. El-Mohandes, Mitigation of voltage sag in a distribution system during start-up of water-pumping motors using superconducting magnetic energy storage: a case study, *J. Energy Storage* 55 (2022) 105441, <https://doi.org/10.1016/j.est.2022.105441>.
- [55] E. Fouladi, H.R. Baghaee, M. Bagheri, G.B. Gharehpétian, A charging strategy for PHEVs based on maximum employment of renewable energy resources in microgrid, in: 2019 IEEE International Conference on Environment and Electrical Engineering and 2019 IEEE Industrial and Commercial Power Systems Europe (EEEIC /I&CPS Europe), Genova, Italy, 2019, pp. 1–5, <https://doi.org/10.1109/EEEIC.2019.8783742>.
- [56] D. Zhang, G. Shafullah, C.K. Das, K.W. Wong, Optimal allocation of battery energy storage systems to improve system reliability and voltage and frequency stability in weak grids, *Appl. Energy* 377 (2024) 124541, <https://doi.org/10.1016/j.apenergy.2024.124541>.
- [57] A. Kumar, A.R. Singh, R.S. Kumar, Y. Deng, X. He, R. Bansal, P. Kumar, R. Naidoo, An effective energy management system for intensified grid-connected microgrids, *Energy Strat.* Rev. 50 (2023) 101222, <https://doi.org/10.1016/j.esr.2023.101222>.
- [58] Bilal Naji Alhasnawi, Basil H. Jasim, A novel hierarchical energy management system based on optimization for multi-microgrid, *Int. J. Electr. Eng. Inf.* 12 (3) (2020). September.
- [59] O. Candra, R. Pradhan, A.N. Shukhratovna, et al., Optimal Day-Ahead Energy Scheduling of the Smart Distribution Electrical Grid Considering Hybrid Demand Management, *Smart Grids and Energy* 9 (2024) 31, <https://doi.org/10.1007/s40866-024-00212-6>.
- [60] Bilal Naji Alhasnawi, Basil H. Jasim, A new energy management system of on-grid/off-grid using adaptive neuro-fuzzy inference system, *J. Eng. Sci. Technol* 15 (2020) 3903–3919.
- [61] A. Nawaz, D. Wang, A. Mahmoudi, M.Q. Khan, X. Wang, B. Wang, X. Wang, MPC-driven optimal scheduling of grid-connected microgrid: Cost and degradation minimization with PEVs integration, *Electric. Power Syst. Res.* 238 (2024) 111173, <https://doi.org/10.1016/j.epsr.2024.111173>.
- [62] E. Fouladi, H.R. Baghaee, M. Bagheri, G.B. Gharehpétian, Power management of microgrids including PHEVs based on maximum employment of renewable energy resources, *IEEE Trans. Ind. Appl.* 56 (5) (2020) 5299–5307, <https://doi.org/10.1109/TIA.2020.3010713>, Sept.-Oct.
- [63] N. Pamuk, U.E. Uzun, Optimal allocation of distributed generations and capacitor banks in distribution systems using arithmetic optimization algorithm, *Appl. Sci.* 14 (2) (2023) 831, <https://doi.org/10.3390/app14020831>.
- [64] L. Li, X. Fan, K. Wu, K. Sethanan, M. Tseng, Multi-objective distributed generation hierarchical optimal planning in distribution network: Improved beluga whale optimization algorithm, *Expert Syst. Appl.* 237 (2024) 121406, <https://doi.org/10.1016/j.eswa.2023.121406>.
- [65] B. Abdollahzadeh, F.S. Gharehchopogh, N. Khodadadi, S. Mirjalili, Mountain gazelle optimizer: a new nature-inspired metaheuristic algorithm for global optimization problems, *Adv. Eng. Software* 174 (2022) 103282, <https://doi.org/10.1016/j.advengsoft.2022.103282>.